Conclusions: The factors most closely associated with ordering deeper levels on skin specimens include small specimen size (0.5 cm or less), punch biopsies, specimens submitted whole, and those with a clinical impression of cancer or dysplasia. We conclude that prospective ordering of deeper levels on such specimens and/ or sectioning specimens currently submitted whole, will improve turnaround time by decreasing the delays encountered when ordering deeper levels after initial review.

1642 Using a Business Review and Scorecard To Manage the Business of Surgical Pathology

LM Yerian, DE Priganc, AE Bennett, G Goss, JL Hunt. Cleveland Clinic, Cleveland, OH; Orion Advisory, LLC, Charlotte, NC.

Background: Surgical Pathology operations can be extremely complex and a variety of factors impact performance. These include personnel, processes, technology, and a host of external pressures. In the business of pathology, these factors must be managed to ensure optimal performance, including clinical service, quality, financial indicators, and productivity. Tools exist in the business arena to manage such performance metrics, but they have not been widely adopted in medicine and are particularly absent in pathology.

Design: We developed a Surgical Pathology scorecard through a collaborative group process. The scorecard tracks data for 15 key volume metrics and 44 performance-related metrics in four categories: Service, Employee Satisfaction and Teamwork, Quality/Risk/Innovation, and Productivity/Financial. A target was set for each metric and performance against the targets discussed in a monthly business review meeting of laboratory supervisors and medical directors, a data analyst, an informatics specialist, the quality officer, and the administrative and physician leadership of Surgical Pathology. Identified gaps between targeted and actual performance levels for a given metric, were analyzed, and a plan to close the gap was developed and implemented.

Results: At the time of scorecard development, only 18% of the metrics were at target. One-year later, most metrics have shown positive trends towards closing gaps, with 58% of the metrics now meeting target. One major benefit of this tool is that it allowed us to quickly recognize increases in the surgical pathology workload and take decisive action to ensure continued efficient and effective laboratory operation .

Conclusions: The performance metric scorecard and monthly business review meeting are very effective management tools for surgical pathology. These tools enable identification and response to trends in key volume metrics. They also enable the surgical pathology leadership to identify metrics that are critical to operational success and to manage performance gaps between current and target values. These tools are excellent for managing productivity, quality, and patient safety data.

1643 Just-in-Time Surgical Pathology Specimen Workflow with Comprehensive Barcode Tracking and Lean/Six Sigma Software Design as a Prototypic Next Generation Laboratory Information System for Comprehensive Error Reduction

L Yu, MS Almiski, UJ Balis. University of Michigan Health System, Ann Arbor, MI; Wayne State University Medical School, Detroit, MI.

Background: The laboratory workflow associated with anatomic pathology (unlike clinical labs) has significantly lagged in the use of advanced and automated specimen tracking technology, with pre- and post-analytical error rates associated with asset identification (for requisitions, specimens, blocks and slides), exceeding 1.5 percent of all accessions for combined intra-case and inter-case misidentification. While the majority of errors are detected, the remaining undetected fraction represents a very real and continuous threat as significant diagnoses may be generated from incorrect source material.

Design: Just-in-time barcode tracking of all specimen materials was developed and implemented in one large academic center (MGH) with knowledge gained from this exercise used to refine a more granular and fault-tolerant process at a second institution (U. of Michigan). The refined process benefited from Value Stream Mapping and quantitative pre- and post-analytical quantitative inference of risk analysis, whereby individual process steps were ranked by both severity of having the potential to cause harm and by frequency of occurrence. Subsequently designed software was itself designed according to Lean principles, with use of Extreme Programming (XP) methodology, to mitigate the seven or more forms of waste that occur with inefficient design models. With insights gained from the above, a further refined AP workflow system was made possible, using a three-tier client-server architecture model.

Results: Initial deployment of the aforementioned just-in-time approaches reduced misidentification errors to undetectable levels. Remaining difficulties in workflow were associated with a small (but finite) non-reading rate of generated barcodes -- an issue resolved by the selection of higher fidelity printing technologies for both slide labels and blocks.

Conclusions: Comprehensively barcode-driven workflow developed in concert with just-in-time methodologies for label generation and lean software design can reduce intra-case and inter-case asset misidentification to undetectable limits. This finding alone can easily justify the assertion that automated tracking techniques should become the new standard of care for anatomic pathology lab workflow.

1644 Reduction of Surgical Pathology In-Process Mis-Identification Defects by Bar-Code Specified Work Process Innovation in the Henry Ford Production System

RJ Zarbo, JM Tuthill, R D'Angelo, R Varney, A Ormsby. Henry Ford Health System, Detroit, MI.

Background: Our implementation of a Lean continuous quality improvement initiative in Surgical Pathology (SP) at Henry Ford Hospital, known as the Henry Ford Production System, enabled workers to identify sources of waste, defects & mis-identifications (mis-ID) arising in all phases of production. In advance of implementing a barcode specified approach to workflow with an integrated identification system of barcoded lab tags, blocks and slides, we defined the baseline of defects causing mis-IDs arising from specimen collection to report generation.

Design: The internal mis-ID rate in SP was assessed using a visual data display for all workers to document defects, as described (AJCP 2007;128:423-429) for 3 weeks in July 2006 (baseline) compared to August 2007 after 200 process improvements and an internally developed bar-coded work system was implemented.

Results: We documented a 63% reduction in mis-ID cases from the baseline rate of 1.67% in 2006 (45 defects in 2694 cases) compared to 0.63% in 2007 (18 defects in 2877 cases). The 2 measurement intervals had comparable numbers of specimen parts (4413 v. 4725), blocks (8776 v. 9167) and slides (14,270 v. 17,927). Defects types remaining in 2007 were 14 encountered in the accessioning process, 4 of which involved blocks, 2 in gross tissue exam, 2 in histology affixing wrong labels to slides and 1 from signout pathologist transposing slides when opening the case in the computer. Slide labeling alone accounted for 2 defects and blocks another 4. These 6 slide and block mis-ID defects accounted for 1/3 of the 18 defects. Blocks and slides formerly accounted for 78% of the defects. The rate of mis-ID blocks and slides was reduced by 85%.

Conclusions: The successes here are attributed to: 1) the management approach known as the Henry Ford Production System, where empowered workers redesigned over 200 surgical pathology laboratory processes in 1.5 years in pursuit of tolerating zero defects, 2) implementation of a bar-code system that maintained identity, specified and standardized work from lab tag to report, and 3) worker design of quality control checks at each workcell to eliminate mis-ID defects. While we have shown marked improvement in creating and maintaining identification of specimens and associated information throughout SP processes, 22% of the case mis-IDs were derived from erroneously labeled specimens sent to the lab, thereby uncovering additional external opportunities.

Techniques

1645 Whole Genome Amplification (WGA) by Strand Displacement Amplification Introduces Significant Errors in Copy Number Alternation Calls in 500K Single Nucleotide Polymorphism (SNP) Array Analysis

A Ahmed, WT Huang, A Ewton, Y Zu, J Hagenkord, C Chang. The Methodist Hospital & TMHRI, Houston, TX; Chang Gung Memorial Hospital-Kaohsiung Medical Center, Chang Gung University College of Medicine, Kaohsiung, Taiwan; Weill Medical College of Cornell University, New York, NY; University of Pittsburgh, Pittsburgh, PA.

Background: Recently, limited studies using SNP genotyping micrroarrays have detected cytogenetically-cryptic uniparental disomy (UPD) and copy number alternations (CNA) in cases of MDS and AML. However, prior studies used unsorted bone marrow samples to perform their analysis. To further specifically study the genetic alternations in different lineages of marrow cells in MDS, we aim to use novel integration of multicolor flow cytometry (FCM) sorting and genome-wide profiling using SNP microarrays. This approach, however, is limited by the amount of sorted cells and thus WGA is needed to obtain enough DNA for SNP analysis in some cases.

Design: Four bone marrow samples from MDS patients were fractionated into erythroid (CD71 bright and CD34-), immature myeloid (CD10- and high side-scatter), blastic (CD34+) and lymphoid fractions (CD45 bright and low side-scatter) using FCM sorting. Genomic DNA from the fractionated cells was extracted. About 10 ng of genomic DNA of each fraction was then amplified by WGA using strand displacement amplification. SNP microarray (GeneChip Human Mapping 500K Set, Affymetrix) was performed using paired amplified and unamplified DNA. Analysis was done using CNAG software.

Results: Monosomy 7 and trisomy 8 were detected by SNP array in one case each using either amplified or un-amplified samples. This finding was consistent with conventional cytogenetic study results. UPD region (16q22.1 to 16q23.2) was identified in one case in both amplified and non-amplified samples. Gains of small chromosomal regions were noted in 2 samples with one sample each showing one CNA region using un-amplified DNA. In contrast, numerous gains or losses (ranging from 9 to more than 30 CNAs) of small chromosomal regions (in range of Mega bases) were noted in all samples using WGA amplified DNA.

Conclusions: SNP analyses using WGA amplified DNA identify UPD or numerical changes of large fragments chromosomal regions as reliable as unamplified DNA. However, the WGA approach introduces abundant errors regarding gains or losses of small chromosomal regions likely due to the non-homogenous amplification of certain segments of genome.

1646 Use of Normal B-Cells as a Negative Control Significantly Impacts the Results of ZAP-70 Expression as Detected by Multiparametric Flow Cytometry

S Alexanian, F Chaves, Q Kong, S Song. UCLA, Los Angeles, CA.

Background: ZAP-70 serves as a surrogate marker for immunoglobulin VH mutation status (iVHms) in CLL patients and is widely used in molecular risk stratification of CLL. ZAP-70 expression as detected by flow cytometry was originally defined as being positive if greater than 20%; such results can be seen in about 50% of CLL cases. Although the technology of ZAP-70 detection by flow cytometry has evolved significantly since 2003, it remains extremely challenging due to lack of proper controls, meaningful thresholds, and standardized analysis and reporting of results. Most labs use T/NK-cells, where ZAP-70 is constitutively expressed, as the positive and sole control for ZAP-70 levels in neoplastic B-cells. Consequently, far more CLL cases are positive for ZAP-70 than the 50% predicted by iVHms. In order to establish consistent quality control standards and provide insight in standardizing the detection of ZAP-70

by multiparametric flow cytometry, a new gating strategy utilizing simultaneous positive and negative controls has been developed at UCLA. Its impact on ZAP-70 results is investigated in this study.
Design: Data was retrospectively collected from 95 CLL patients who had ZAP-70 studies performed between 01/2005 and 09/2007. The ZAP-70 expression for each case was determined by both the more common approach where T/NK-cells are used as a sole positive control (Strategy 1), and our new gating strategy where normal B-cells are added as negative controls (Strategy 2). The results were compared using the student T test.
Results: The average percent of ZAP-70 expression was 41.36% when Strategy 1 was used for data analysis, and 13.86% when Strategy 2 was employed. This difference was statistically significant ($p < 0.001$).
Conclusions: Use of normal B-cells as negative controls, in conjunction with T/NK-cell positive controls, yields dramatically different ZAP-70 results when compared to a traditional gating strategy. This difference is clinically significant as it changes the interpretation of numerous cases from positive to negative. This finding demonstrates the significant impact our new gating strategy has on ZAP-70 results and highlights the critical need for further standardization. In this retrospective study gene sequencing for iVHms could not be assessed; therefore, further studies incorporating such gene sequencing are vital in elucidating the marked differences and standardization of ZAP-70 detection, as well as in comparing the most accurate gating strategy.

1647 Tissue Banking Informatics: Experience from a Multi-Institutional Academic

W Amin, SK Mohanty, AV Parwani, R Dhir, MJ Becich. University of Pittsburgh, Pittsburgh, PA; University of Pittsburgh School of Medicine, Pittsburgh, PA.
Background: Tissue Banking Informatics deals with standardized annotation, collection and storage of biospecimens that can further be shared by researchers. Over the last decade, the department of Biomedical Informatics at the University of Pittsburgh took an initiative in configuring various tissues banking informatics models to expedite translational medicine. Here we describe the components and scopes of these models.
Design: For clinical annotation of biospecimens the data is retrieved from various hospital based systems: (a) Pathology laboratory Information System - coPath Plus (Cerner) and synoptic templates for surgical pathology specimens; (b) Cancer Registry Information System; and (d)Tissue Bank Inventory System. Data is de-identified by honest broker or by employing De-ID® application. Based upon these components the UPMC with its collaborators have developed various organ specific as well as federated biosrepositores. These Organ specific models are developed on Oracle 9.2.0.1 Server to generate dynamic pages for the database. The federated model is based on the innovation of soft and hardware technology by National Cancer Institute's cancer Biomedical Informatics Grid by utilizing Java applications and information model.
Results: The organ specific biorepositories include Cooperative Prostate Cancer Tissue Resource, Pennsylvania Cancer Alliance Bioinformatics Consortium, Colorectal, Head & Neck, Hematolymphoid and Mesothelioma biobanks. The federated models includes the caTISSUE Core - a centralized tissue bank, the cancer Text Information Extraction System for extracting valuable information from the archival pathology surgical reports and the caTISSUE Clinical Annotation Engine. These biorepositories provide thousands of well annotated biospecimens for the researchers.
Conclusions: The systems provided by Tissue Banking Informatics ultimately form a common platform for cancer research to accelerate advancements in clinical and translational research. In addition, the various tools utilized by these systems provide a tangible infrastructure and resource for education and clinical services within the laboratory information system. Furthermore, applications developed within the tools will provide a novel method to add value to the existing clinical document, archives, and biospecimens.

1648 An Informatics Supported Web-Based Data Annotation and Query Tools To Expedite Translational Research for Head and Neck Malignancies: An Update

W Amin, AT Mistry, H Singh, JR Hetrick, SK Mohanty, AV Parwani. University of Pittsburgh, Pittsburgh, PA.
Background: Advancement in translation medicine and the increasing requirement of biomarker validation studies directed the need for high quality biospecimens with standardized clinicopathological annotation. One such initiative is the virtual biorepository for head and a neck neoplasm which is a bioinformatics supported system to incorporate data from various clinicopathology and molecular systems into a single architecture carried out through a set of common data elements (CDEs) in order to fulfil the growing needs of researchers. This system provides semantic and syntactic interoperability of datasets across multiple institutions.
Design: The warehouse provides a web-based data annotation and query engine supported in a three-tiered architecture, and implemented on an Oracle Application Server on a Compaq DL360 Server running Win2K with SP. The application utilizes the Oracle http server and mod_plsql extensions to generate dynamic pages from the database to the users. The database is the Oracle 9.2.0.1 Enterprise Edition implemented on a SunFire V880 Server running Solaris 2.8. The annotation tool incorporates CDEs developed *from* the College American Pathologist Checklist and North American Association Central Cancer Registry standards for head and neck neoplasms. The data annotation engine is a portable, flexible and web based data entry device, while the data query engine allows to search de-identified information within the warehouse through a "point and click" interface.
Results: The head and neck database contains multimodal datasets that are accessible to researchers via an easy to use query tool. The database currently holds 6326 cases and 10322 tumor accessions with annotation. Included among these are 1238 metastatic cases, 3992 primary, 1857 recurrence, 572 new primary and 123 unknown primaries. The data disclosure is sterically regulated by user's authorization.
Conclusions: The head and neck neoplasm virtual biorepository with robust translational biomedical informatics support to facilitate basic science, clinical, and translational research. The Head and Neck data query tool acts as a central source providing a mechanism for researchers to efficiently and effectively find clinically annotated datasets and biospecimens relevant to their research areas.

1649 Lineage Infidelity of Nuclear Transcription Factor [Estrogen Receptor (ER), Thyroid Transcription Factor-1 (TTF1), and CDX2] Expression in Identification of Carcinomas

GS Baird, LC Goldstein, AM Gown, CE Bacchi, PL Kandalaft, TS Barry. PhenoPath Laboratories, Seattle; Consultoria em Patologia, Sao Paulo, Brazil.
Background: Immunohistochemistry (IHC) for lineage-specific markers, especially nuclear transcription factors, is used to determine a likely site of origin of carcinomas of unknown primary presenting as metastases. However, the specificities of these markers have been incompletely studied. In this study, antibodies to ER, TTF1, and CDX2 were applied to primary carcinomas of the breast, lung, and colon, in order to determine their specificity. Two clones of anti-TTF1 antibodies were also compared to investigate the dependency of specificity on the antibody clone employed.
Design: Biopsies or resection specimens from 124 breast, 55 colonic, and 42 lung non-small cell clinical primary adenocarcinomas (all whole sections except 10 lung adenocarcinomas that were part of tissue microarrays) were stained for ER (Lab Vision, SP1 clone), CDX2 (Biogenex clone CDX2-88), and TTF-1 (Novocastra clone SPT24 and Dako clone 8G7G3/1) by IHC using standard detection methodology. Staining of each marker was scored semi-quantitatively.
Results: In general, detection of nuclear transcription factors was found to be highly specific for confirming tissue origin of primary carcinomas. The table below enumerates the sensitivities and specificities for each clone for selected carcinoma types.

Nuclear Transcription Factors Staining by IHC

	Fraction (Percent) Staining			
Primary Carcinoma Site	TTF-1 (SPT24)	TTF-1 (8G7G3/1)	ER	CDX2
Breast	0/124 (0)	0/124 (0)	103/124 (83)	0/124 (0)
Colon	7/55 (13)	1/55 (2)	0/55 (0)	41/55 (75)
Lung	32/42 (76)	22/42 (52)	2/42 (5)	0/42 (0)

SPT24 showed the most cross reactivity, to colon carcinomas, and colonic carcinomas were more frequently aberrantly stained than the other two carcinoma types. SPT24 is significantly more likely to identify TTF-1 in primary colon carcinomas than the clone 8G7G3/1 ($p=0.03$, Fisher's exact test).
Conclusions: Nuclear transcription factors are useful for differentiating tissue lineage in a set of breast, lung, and colon primary non-small cell carcinomas, with overall specificities exceeding 95% for all antibody clones except SPT24 used to identify TTF-1. These results suggest that IHC for nuclear transcription factors should be highly specific for discriminating between breast, colon, and lung primary carcinomas in the setting of metastases from tumors unknown origin, although some lineage infidelity does exist.

1650 Digital Analysis of Congo Red Stained Fat Pad Aspirate Specimen: A Capable Tool in the Diagnosis of Systemic Amyloidosis

S Bardarov, C Michael, R Pu, Y Pang. University of Michigan, Ann Arbor, MI.
Background: Abdominal fat pad fine needle aspiration (FNA) has been utilized since 1970 with comparable efficacy. Positive specimens are focally "salmon pink" by light microscopy, with "apple green" birefringence on polarization. Correct recognition of the polarizable green color is critical for a diagnosis. When it is focal, the color can be misinterpreted leading to a wrong diagnosis. This study explored and demonstrated the usage of digital analysis to accurately recognize the polarizable green color to enhance the diagnosis of systemic amyloidosis.
Design: Congo Red stained tissue sections (12) of previously confirmed systemic amyloidosis various organs and negative cases of fat pad aspirate (7) were selected for the study. Digital images were captured through polarizing microscopy with digital camera (Insight 4.2) and software (Spot) both from Diagnostic Instrument Inc. The images were analyzed with Adobe Photoshop SC3 by selecting the interested area, measuring the parameters in each channel of blue and green and characterizing the colors with the ratio of Green:Blue (G:B). The data were imported into Microsoft Excel. The value of G:B ratio considered to be positive was determined from the accumulated data of the positive cases. The mean G:B ratio of interesting color areas in the positives and negatives was compared. Eleven cases with previously established diagnosis were analyzed using this method.
Results: A total of 953 areas from images of selected amyloidosis cases were analyzed to reveal the mean G:B to be 2.090 with a standard deviation of 0.205. While in 387 interesting color area of negative cases the mean G:B was 1.700 with SD 0.229. The means from these two populations are significantly different (P value < 0.0001). We determined that the cutoff value of G:B for a positive color area should be G:B $\geq$1.9, which will recognize 82% positive and 96% negative cases correctly. We successfully confirmed 5 positive cases and recognized 6 negative cases using this method. The diagnoses were all in concordance with concurrent biopsies or clinical follow-up information.
Conclusions: Digital analysis is a capable tool to assist the diagnosis of systemic amyloidosis on fat pad fine needle aspiration specimens. It is applicable and especially useful with fat pad aspirate specimens.

1651 Expression of ATM Gene Product in Human Malignant Neoplasms

MD Begnami, M Ventura, LF Reis, FA Soares. Hospital AC Camargo, Sao Paulo, Brazil.

Background: The ATM (ataxia telangiectasia mutated) kinase plays an essential role in maintaining genome integrity by coordinating cell cycle, arrest, apoptosis and DNA damage repair. ATM gene is located on chromosome 11q22-23 and loss of protein expression is associated with gene mutations. ATM gene mutated has been associated with tumorigenesis of many different tumors. The effect of ATM protein loss on tumor multiplicity is largely independent of the effect of ionizing radiation. Very little is known about the expression of ATM protein in human cancer. To address this issue, we examined the expression pattern of ATM protein in a group of malignant tumors.

Design: 250 malignant tumors were subjected to immunohistochemistry by using antibody for ATM protein (Y 170, Epitomics), according with the manufatures guidelines. Tumors were arranged in a multitumor tissue microarray, containing 25 cases of each tumor: mammary, pancreatic and prostatic adenocarcinomas, retinoblastomas, melanomas, gliomas, neuroblastomas, neuroendocrine tumors and squamous cell carcinomas of head and neck (SCCHN). High ATM protein expression was considered when nuclear positive was observed in more than 5% of the tumor cells.

Results: High ATM protein expression was observed in 5/19 (26%) mammary adenoca, 8/17 (47%) prostatic adenoca, 6/17 (35%) pancreatic adenoca, 17/18 (94%) retinoblastomas, 14/21(66%) melanomas, 13/17 (76%) neuroblastomas, 14/19 (74%) gliomas, 9/13 (70%) SCCHN and 6/21 (29%) neuroendocrine tumors.

Conclusions: We provide evidence suggesting that (1) loss of ATM protein expression is a common finding in epithelial and neuroendocrine tumors; (2) attenuation of ATM function may be an important event in the progression of tumors with high ATM protein expression. Studies in tumors from large scale are now necessary to validate our data and establish the ATM gene participation in human carcinogenesis, which warrants further investigation.

1652 Virtual FISH Using the UroVysion Assay

KJ Bloom, H Vall, T Ha, S Chen. CLARiENT, Inc, Aliso Viejo, CA.

Background: Virtual pathology has been widely accepted for the analysis of breast prognostic markers and flow cytometry samples but to date has not been used for FISH analysis. UroVysion is an FDA cleared FISH assay which simultaneously assesses the ploidy status of three chromosomes and looks for the deletion of the p16 gene. When used with cytology and cystoscopy it can significantly improve the early detection of recurrent bladder cancer and in the correct clinical setting, it may serve as an aid to the early detection of bladder cancer. We present a method that enables the pathologist to remotely interact with an FDA cleared software system over the internet, allowing the pathologist to select and analyze the appropriate cells.

Design: 211 select urine samples were sent to a reference laboratory for Urovysion analysis (Abbott Molecular Inc.,Des Plaines, IL). The urine was prepared according to the manufacturer's guidelines, the slides hybridized with the UroVysion probes, and the resulting slides digitally scanned and individual cells classified using the BioView Duet Imaging Station (BioView, Israel). We modified the BioView Solo imaging workstation, used to review and analyze the individual captured cells, using Remote Access terminal services (Microsoft Corp, Washington). The Solo workstation was then made accessible via the internet using Internet Explorer, v7.0.

Results: 211 UroVysion samples were prepared in California and reviewed remotely by pathologists at a distance of over 2500 miles. In 191 of these cases (90.5%), the reviewing pathologist was satisfied with the clinical findings and the digital review of the slide. In the remaining 20 cases, the reviewing pathologist was uncomfortable with interpreting the results remotely and required that the entire slide be reviewed under a fluorescent microscope before issuing a report.

Conclusions: This study showed that it is possible to perform virtual microscopy on FISH samples in select circumstances. This system may allow local pathologists without access to their own FISH laboratory, the ability to perform the professional interpretation of FISH slides and remain actively engaged in the care of their patients.

1653 Quantitation of Phosphoproteins in Fixed Tissue Samples Using Quantum Dots

J Bodo, R Steinle, R Haney, ED Hsi. Cleveland Clinic, Cleveland, OH.

Background: Phosphoproteins (PPs) are important in mediating signal transduction pathways. Many therapeutic candidates target these pathways. Thus, the *in situ* quantitative measurement and subcellular localization of PPs will likely be important in predicting response to these agents. We are in the process of validating an automated Quantum dot (Qdot) based immunofluorescent (IF) assay applicable in fixed tissues that will allow retrospective PP quantitation.

Design: UT7/EPO, HEL, and HT-29 cells served as a model cell lines. Dynamic range of quantitative assays was tested by activation of several kinases using erythropoietin, IGF-1 and hydrogen peroxide. In order to most closely mimic biopsy specimens, we used SCID mouse xenografts of HEL and HT-29 cells to generate human cell line tumors with defined PP profiles. PPs were detected by IF using phosphospecific antibodies, biotinylated secondary antibodies, and streptavidin Qdot605 and quantitated by commercial imaging software. Western blots of paired samples served as the standard.

Results: In cultured UT7/EPO cells, erythropoietin stimulation led to the rapid phosphorylation of ERK1/2 (T202/ Y204) and STAT5 (Y694), which decreased in a time dependent manner. In cultured HEL cells, oxidative stress induced by hydrogen peroxide caused a strong phosphorylation of ERK1/2 kinases. IGF-1 and hydrogen peroxide treatment modulated various levels of phospho-AKT (S473) in HT-29 cells. Furthermore, high amplification of phospho-AKT levels was seen in HT-29 xenografts after IGF-1 injection. Loss of PP signal (pSTAT5, pAKT, pERK1/2) due to delay in fixation was studied in xenograft sections at various time points (0 – 120 min) to mimic pathology laboratory practice. Using data from all experiments, repeated models were used to estimate levels of phosphorylation at each condition level, and estimate the variability in fluorescence within and between experiments. Our studies show that Qdot IF quantitation in tissue sections correlates well with Western blot data (R>0.8).

Conclusions: These results indicate that Qdots can be very effective in quantitation of PPs and offer several advantages over organic dyes. Taken together, Qdot technology offers a novel technique for quantitative examination of PPs in fixed tissues. However, time dependent changes in PP prior to fixation highlight the importance of rapid processing.

1654 High Definition Video Recording of Surgical Pathology Dissections: A Useful Tool for Medical Student Education

K Boland, C Brady, J Woosley. University of North Carolina Shool of Medicine, Chapel Hill, NC.

Background: Gross pathology is a critical link between the clinical presentation of a patient and the histopathology of their disease. Medical students acquire this body of knowledge through photographs of gross specimens and through archived, formalin-fixed specimens. Gross photographs of unfixed specimens can be helpful in that they can present the pathology in realistic color. However, photographs are static and two-dimensional, limiting a student's ability to understand pathologic processes. Archived, formalin-fixed specimens retain three dimensions, but colors in the specimen are unrealistic and these specimens can deteriorate badly with time and use. Additionally, many students find these fixed specimens unpleasant to handle and often prefer to simply watch a pathology instructor demonstrate the gross pathologic features.

Design: The goal of this project was to use new and inexpensive technology to help medical students develop an understanding of gross pathologic changes in diseased organs. A high quality consumer digital video camera was paired with an external directional microphone to record gross dissections of active surgical pathology cases. An informal, conversational-type narration accompanies each recorded dissection. Edited gross pathology dissection videos were used to create menu-driven DVDs, organized by organ-system.

Results: Approximately 100 video gross pathologic demonstrations have been created, covering a broad range of diseases. These video demonstrations show pathologic process with stunning clarity of detail and are augmented by a descriptive audio narration. High definition video recordings of gross pathology dissections are introduced into the second year medical student integrated GI organ system course as an educational trial.

Conclusions: High definition, narrated video recordings of pathologic specimens examined in the surgical pathology grossing area can become a valuable teaching resource, greatly enhancing the pathology educational experience of our medical students. This resource can be created with a minimal investment in time and equipment. Gross pathology videos can be viewed on computer screen or on either standard or high definition TV. Videos can also be viewed on pocket-sized media-capable devices (i.e., video iPod) to increase the portability of the educational experience.

1655 Microarray Method for the Detection and Localization of Balanced Chromosomal Rearrangements

WR Burack, M Heinz, SD Crosby, JD Pfeifer. University of Rochester, Rochester, NY; Washington University in St. Louis, St. Louis, MO.

Background: Microarray techniques, such as Comparative Genomic Hybridization, do not detect balanced translocations and inversions or any other type of copy-number neutral structural rearrangements. We describe a method which combines oligonucleotide microarray technology with Fluorescence-In-Situ Hybridization performed on the microarray (FISH-on-Chip) for identification of copy-number neutral chromosomal rearrangements with precise identification of involved breakpoints.

Design: This FISH-on-Chip method uses the microarray to capture DNA fragments containing sequences adjacent to a chromosomal breakpoint, and a FISH probe to identify sequences on the captured fragments that are derived from the second chromosome involved in the translocation. The location on the array of the bound FISH probe precisely localizes the chromosomal breakpoint. We modeled detection of a balanced chromosomal translocation with a 300 bp construct representing the t(12;16)(q13;p11) found in angiomatoid fibrous histiocytoma.

Results: Sequence Specificity: A construct containing the t(12;16) was mixed with excess total human DNA and annealed directly the microarray. The bound construct was then detected with the fluorophore-tagged BAC probe representing the region of human chromosome 16 known to be involved in this translocation. The chromosome 16 probe annealed specifically to the chromosome 12 feature involved in the tranlocation: of 237,366 evaluable features in two successive experiments, 24 and 114 features had signals >6 SD above the mean in the replicates, but none of the features other than those represented in the t(12;16) translocation had a signal >1 SD above the mean in both experiments. Sensitivity: The translocation construct was diluted 10^7 in total human DNA to obtain the molar ratio expected in a diploid tumor specimen. Using replicate experiments, this dilution of construct could be reliably detected (p=0.030). Multiplex: A construct representing an inversion of chromosome 12 (inv12) and a construct representing a deletion of chromosome 16 (del16) were produced. These rearrangements could be simultaneously detected in a single study.

Conclusions: The method is sufficiently sensitive for multiplexed diagnostic studies and is amenable to high resolution whole genome discovery projects.

1656 The Detection and Characterization of the Abnormal Plasma Cells in B Cell Lymphoproliferative Disorders with Plasmacytic Differentiation by Six-Color Single Tube Flow Cytometry

D Chen, WG Morice. Mayo Clinic, Rochester, MN.

Background: The detection of the plasmacytic component in B-cell lymphoproliferative disorders with plasmacytic differentiation (LPDP) such as lymphoplasmacytic lymphoma

(LPL) is essential. However, these plasma cells (PC) may be small in number and their phenotype has not been well characterized. In this study, we demonstrated that a recently described six-color single tube flow cytometry method (Morice W.G. et. al. Leukemia 2007) also sensitively detects and characterize the abnormal PCs in LPDP.
Design: Fifteen specimens (14 bone marrows and 1 thyroidectomy), involved by LPDP (8 LPL, 2 IgM MGUS, 5 low grade B-cell LPDP) were analyzed. The clinical and laboratory data were reviewed. Four color flow cytometric immunophenotyping were performed in each case using antibodies to CD3, CD5, CD10, CD11c, CD16, CD19, CD20, CD22, CD23, CD38, CD103 and surface kappa and lambda immunoglobin (Ig) light chains. PC analyses were performed by a six-color single tube method using antibodies to CD19, CD38, CD45, CD138, cytoplasmic kappa and lambda Ig light chains as previously described (Morice W.G. et. al. Leukemia 2007). Paraffin section immunohistochemical studies were performed on some cases using antibodies to CD3, CD20, Pax5, CD138 and kappa/lambda Ig light chains.
Results: All patients (median age 66, range 42 to 83 years) had abnormal serum monoclonal IgM protein (median 2.0 g/dL, range 0.5 to 4.2 g/dL). The presence of both abnormal B-cells and PCs were confirmed by the morphological examination and immunohistochemical studies on the paraffin sections. The clonotypic B-cells were detected in all cases by four-color flow cytometry, which however was unable to identify the abnormal PCs. In contrast six color flow cytometry identified an abnormal PC component in all LPDP. These PCs were cytoplasmic Ig light chain restricted and were typified by bright co-expression of CD38 and CD138. In each case the PCs of LPDP expressed CD19 and CD45, this is in contrast to the PCs of multiple myeloma (MM) which are typically CD19 negative and show variable CD45 expression.
Conclusions: Single tube six-color flow cytometry sensitively detects and characterizes the abnormal PCs of LPDP. While these PCs in LPDP have phenotypic overlap with the abnormal PCs of true plasma cell proliferative disorders as MM, they are more closely related to true B-cells. Hence, 6-color flow cytometry can serve as a valuable tool in establishing a diagnosis of LPDP.

1657 Critical Evaluation of D2-40 (Podoplanin) from Two Vendors in Relation to the Differential Diagnosis of Mesothelial Lesions

K D'Amore, G Varsegi, M Goswami, G Dawson, VB Shidham. Medical College of Wisconsin, Milwaukee, WI.
Background: D2-40 has shown promise as an immunomarker for mesothelial cells. Its immunoexpression in other lesions and tissues including germ cell tumors, granulosa cell tumors, ovarian serous carcinomas, and lymphatic endothelium are being reported. These studies used the Signet® monoclonal antibody. In the current study we compared this antibody with the same clone from Dako®.
Design: We studied 86 well-differentiated carcinomas (21 breast, 20 colon, 20 pulmonary, 25 pancreatic), 7 pleural mesotheliomas, and 15 specimens with reactive mesothelium (5 pleura, 5 pericardium, 5 hernia sac). Initial diagnoses over 4 years period were based on H&E and selective immunostains. Three consecutive sections of formalin fixed, paraffin embedded tissue blocks [1. HE stain, 2. Signet D2-40 immunostain (1:100 as per package insert), and 3. Dako D2-40 immunostain (1:200)] were evaluated. Other immunostaining variables, including antigen retrieval with HIER at pH 6, were the same for both antibodies. Immunostaining pattern and intensity were analyzed.
Results: 1. Both mesothelioma cells (7) and reactive mesothelial cells (15) were immunoreactive in all cases (22/22, 100%). Spindle cell components of mesothelioma showed relatively weak cytoplasmic immunoreactivity, without significant membranous staining, as compared to epithelioid areas, which showed prominent membranous immunostaining with a microvillous pattern (better seen under oil immersion). 2. All cases of carcinoma were non-immunoreactive except in foci with squamoid features in two lung adenocarcinomas (2/86, 2.3%). The immunostaining pattern in these two cases was cytoplasmic, with an ill-defined membranous component, and without distinct microvilli. 3. Dendritic cells, lymphatic endothelium, peripheral nerves, chondrocytes, myoepithelial cells in breast, basal cells in bronchial mucosa, and pneumocytes also demonstrated D2-40 immunoreactivity. 4. Both antibodies showed similar results. However, the immunostaining with Signet was darker than Dako's.
Conclusions: 1. D2-40 is a specific immunomarker for both reactive and neoplastic mesothelial cells. 2. Lack of membranous immunostaining with a conspicuous microvillous pattern favors a non-mesothelial origin, and is very useful in the differential diagnosis of lung carcinoma. 3. Reactive dendritic cells in desmoplastic stroma in tumors may be distracting. The Dako antibody's lighter immunostaining reduced the intensity of this interference. 4. Results with Signet and Dako were comparable.

1658 Multiplex Nucleic Acid Amplification Assay for the Detection of 15 Human Respiratory Viruses

AF Durden, DV Spencer, DJ Wolff, LL Steed, GG Re, L Youngberg. Medical University of South Carolina, Charleston, SC.
Background: Currently, respiratory virus testing is based on viral culture and rapid antigen detection for six to seven common viruses. Limitations of culture techniques include extended turnaround times and suboptimal sensitivity and specificity. Multiplex PCR offers the ability to increase sensitivity, while decreasing the time to result. A rapid PCR test capable of detecting a wide array of viruses would enhance patient management by reducing inappropriate antibiotic use and increasing more efficient allocation of hospital resources.
Design: We used the Luminex Corporation (formerly Tm Biosciences) Respiratory Viral Panel assay (RVP) to test 94 specimens (22 bronchoalveolar lavage samples and 72 nasal washing samples). RVP tests for 15 respiratory viruses (adenovirus, influenza A and B, parainfluenza types 1-4, respiratory syncytial virus [RSV] A and B, enterovirus-rhinovirus, human metapneumovirus, and coronaviruses OC43, 229E, NL63, and HKU1). Multiplex PCR was performed and the labeled products were hybridized to a microsphere-based array and analyzed using the Luminex flow cytometer. PCR results were compared with viral culture results.
Results: Respiratory viruses were detected in 13 (14%) and 34 (36%) specimens by culture and by RVP, respectively. The overall concordance between culture and RVP was 69% (8 specimens positive by both and 57 negative by both). Of the discordant samples, 5 samples were positive by culture and negative by RVP, while 24 were positive by RVP and negative by culture. The increased diagnostic yield of RVP was due to detection of viruses not isolated by culture and mixed viral infections detected by RVP. Single-target PCRs are being performed to verify the RVP results.
Conclusions: The Luminex RVP system provides clinical laboratories with a rapid and sensitive method to detect 15 common respiratory viruses.

1659 Comparison of Whole-Slide Imaging to Robotic Microscopy for Primary Frozen Section Diagnosis by Telepathology

AJ Evans, R Chetty, BA Clarke, S Croul, R Kiehl, B Perez-Ordonez, SL Asa. University Health Network, Toronto, ON, Canada.
Background: Interest in the use of telepathology (TP) in North America for diagnostic purposes is steadily growing. In 2004, we implemented a robotic microscopy (RM) TP system to provide primary frozen section (FS) diagnoses at University Health Network (UHN). Whole-slide imaging (WSI) represents a major technological advance in the area of TP. This study compares our current experience using WSI for primary FS diagnosis to our previous experience with RM.
Design: UHN comprises three sites in downtown Toronto. Pathology services are consolidated at the Toronto General Hospital (TGH) site. The Toronto Western Hospital (TWH) has no on-site pathologist, but requires FS support at the rate of 1-10 cases/week. From November 2004 to September 2006, FS diagnoses at TWH were made by TP using RM. We replaced the RM system with WSI in October of 2006. FS slides are now scanned at 20x by TWH histotechnologists to create compressed JPEG files. Pathologists located at TGH access the scanned slides via the UHN intranet, view them on their office computers and communicate the FS diagnoses directly to the TWH surgeon by telephone.
Results: We have used TP to make 674 primary FS diagnoses (350 by RM and 314 by WSI), 95% of which were for neurosurgical cases. Pathologists required an average of 9.98 minutes to review a FS slide by RM. This time decreased to an average of 2.71 minutes/slide using WSI, with 26% of cases requiring < 1 minute/slide and 43% of cases < 2 minutes/slide. Smears were examined in addition to FS slides in 30% of the WSI cases. An average of 4.43 minutes was required to review both the FS and smear slides. The average file size was 35.7 Mbytes/slide (range 3.7-180.0) for FS slides and 132.2 Mbytes/slide (range 23.0-293.6) for smears. Diagnostic accuracy was 98% for both WSI and RM, however the use of WSI has markedly improved pathologist satisfaction when making FS diagnoses by TP. WSI also readily facilitates consultation with colleagues on difficult cases.
Conclusions: WSI has resulted in a 3.7-fold reduction in the time required to review a FS slide by TP when compared to our previous RM system. While diagnostic accuracy has remained the same, pathologist satisfaction has markedly improved following the implementation of WSI.

1660 Web-Based Pathology Tumor Reporting System with Enhanced Data Collection, Re-Usability and Storage

JJ Findeis-Hosey, T Ikpeze, Y Mao, DM Hosey, C Van Vranken, Z Qu. University of Rochester Medical Center, Rochester, NY.
Background: Accurate pathology reporting of a wide variety of malignant tumors has increasingly become a complex task. Innovative and efficient tools can greatly simplify the reporting process and minimize reporting errors. We previously introduced a web-based tumor reporting system (Qu, et al., AJCP 127:898, 2007). We now report several improvements, specifically 1) client control of data collection/storage by including a web data download function, 2) data re-usability by seamlessly incorporating SNOMED-CT and ICD-9 codes, 3) multiple formats for final pathology reports, and 4) structural flexibility for easy update of content and functionality (such as multi-language capability).
Design: We created a dynamic Microsoft Active Server Page (ASP.NET) web-based tumor reporting system using Microsoft Visual Web Developer (VWD). Organ-specific tumor templates were created containing drop-down list and data-compile features. Microsoft Access databases are used to populate each organ-specific template with pre-defined data elements. Corresponding SNOMED-CT and ICD-9 codes are coupled with the pre-defined data elements. User input can be viewed in a variety of reporting styles or downloaded as discrete data elements in a Microsoft Access database.
Results: The reporting system is freely accessible on the Internet. Reporting elements of required data categories for each organ/site are presented as drop-down lists in tumor reporting templates by an Internet browser. The data elements, selected by the web user based on pathology findings, are compiled with embedded SNOMED-CT and ICD-9 codes into a concise and uniform output format/style which can then be 1) transferred to a local laboratory system as en-bloc text by copy-paste and/or 2) saved into a local database as discrete data elements for future use by the local user. The web data components are permanently purged out when the browser is terminated. The system and reporting process are HIPPA compliant. New templates or data elements can be easily incorporated into the system. Multi-language capabilities allow for international use.
Conclusions: The improved tumor reporting system 1) makes routine pathology tumor reporting more efficient, 2) enhances data usability by incorporating SNOMED-CT and ICD-9 codes, 3) gives the web user full control of data collection, local storage, and data security, and 4) allows easy and prompt update of its contents to meet changes in reporting requirements.

1661 Elevated Hydrostatic Pressure Promotes Protein Recovery from Formalin-Fixed, Paraffin-Embedded Tissue Surrogates

CB Fowler, RE Cunningham, TJ Waybright, J Blonder, TD Veenstra, JT Mason, TJ O'Leary. Armed Forces Institute of Pathology, Rockville, MD; Veterans Health Administration, Washington, DC; National Cancer Institute, Frederick, MD.

Background: High-throughput proteomic studies on formalin-fixed paraffin-embedded tissues have been hampered by inefficient methods to extract proteins and by an incomplete knowledge of formaldehyde-induced protein modifications.

Design: Lysozyme tissue surrogates were prepared as previously described, deparaffinized, and rehydrated through graded alcohols. Cleared surrogates were then incubated in distilled water for 30 minutes, homogenized with a pellet pestle followed by sonication, then heated in a water bath at 80°C for 2 h at ambient pressure, or processed for various times under elevated temperature and pressure and extracted at 45,000 psi and 80–100°C in Tris buffers containing 2% SDS and 0.2 M glycine at pH 4. Protein concentrations were determined spectrophotometrically; the protein composition of the solublized fractions was characterized by SDS-PAGE. Surrogate samples were analyzed by reversed phase liquid chromatography coupled directly in-line with a hybrid linear ion-trap Fourier transform mass spectrometer equipped with a nanoelectrospray ion source and operated in a data-dependent mode where the seven most intense ions detected in each MS scan were selected for tandem MS in the linear ion trap. The peptide searches were conducted allowing for up to two internal missed tryptic cleavage sites.

Results: Reversal of formaldehyde-induced protein adducts and cross-links was seen when surrogates were extracted at 45,000 psi and 80–100°C in Tris buffers containing 2% SDS and 0.2 M glycine at pH 4. These conditions also produced peptides resulting from acid-catalyzed aspartic acid cleavage. Additives such as trimethylamine N-oxide or copper (II) chloride decreased the total percentage of these aspartic acid cleavage products, while maintaining efficient extraction of de-modified protein from the FFPE tissue surrogates. Mass spectrometry analysis of the recovered lysozyme yielded 70% sequence coverage, correctly identified all formaldehyde-reactive amino acids, and demonstrated hydrolysis at all of the expected trypsin cleavage sites.

Conclusions: Elevated hydrostatic pressure treatment is a promising approach for improving the recovery of proteins from FFPE tissues for proteomic analysis.

1662 Capillary Zone Electrophoresis (CZE) Is an Efficient and Accurate Method for Variant Hemoglobin Analysis: A Study of 662 Patients Comparing CZE and High-Performance Liquid Chromatography

ME Gorospe, DL Cruser, AW Taylor, SS Collins, JA Vos. Wilford Hall Medical Center, Lackland AFB, TX; Brooke Army Medical Center, Fort Sam Houston, TX.

Background: Analysis of hemoglobin variants by ion-exchange high-performance liquid chromatography (HPLC) and gel electrophoresis is well-established. The relatively new technique of capillary zone electrophoresis (CZE) is reported to have higher throughput but has not been fully evaluated for hemoglobin analysis.

Design: We compared HPLC to CZE on 662 consecutive patient samples. Correlation coefficients were determined for percentages of hemoglobins A, A_2, F, S, and C. All abnormal hemoglobin identities were confirmed by agarose and citrate gel electrophoresis.

Results: All abnormal hemoglobins identified by HPLC were detected by CZE and one additional hemoglobin variant (Constant Spring trait) was detected by CZE only (N=86, 13%, diagnostic correlation 99%). Correlation coefficients in normal patients (n=576, 87%) were greater than 0.908 (A: 0.982, A_2: 0.908, F: 0.998) when comparing the two methods. Abnormal hemoglobin (n=86, 13%) percentage levels (S, C, E, H, City of Hope, G-Philadelphia, Lepore) had a composite correlation coefficient of 0.987. However, among one of the most common variants (ie, diseases involving hemoglobin S, n=72, 11%), correlation coefficients were greater than 0.992 for all hemoglobins except for A_2 (A: 0.999, A_2: 0.511, F: 0.996, S: 0.992). The poor correlation of A_2 in this group is likely due to hemoglobin S degradation products that are known to co-elute with the A_2 peak on HPLC (seen in 56/72 [78%] cases with hemoglobin S). This finding was not observed in any of these patients when analyzed by CZE. Correlation coefficients for beta thalassemia patients (n= 25, 3.8%) were greater than 0.912 (A: 0.963, A_2: 0.912).

Conclusions: In addition to the potential gains in efficiency (34 samples/hour on CZE versus 6 samples/hour on HPLC), CZE offers improved peak resolution of hemoglobin A_2, especially in the presence of hemoglobin S, and is equivalent to or better than HPLC in diagnosing hemoglobinopathies and thalassemia. Capillary zone electrophoresis appears to be an attractive alternative to HPLC for hemoglobin analysis in laboratories with high throughput requirements.

1663 Confirmation of Abnormal BAC Array Comparative Genomic Hybridization (array CGH) Results Using High Resolution Oligonucleotide Arrays

RA Higgins, SR Gunn, RS Robetorye. The University of Texas HSC at San Antonio, San Antonio, TX; Combimatrix Molecular Diagnostics, Irvine, CA.

Background: Array CGH is a powerful diagnostic tool with applications for the identification of genetic alterations in cases of developmental delay-mental retardation (DD-MR). Unlike fluorescence in situ hybridization (FISH), in which the choice of diagnostic locus-specific probes is based on clinical features and differential diagnosis, BAC CGH arrays detect genome-wide chromosomal imbalances with probes targeting regions of the genome that are altered in the most common congenital abnormalities. While BAC array CGH has proven to be a highly effective method for identifying cryptic chromosomal aberrations, it is still recommended that genetic alterations identified by array CGH be subsequently confirmed by another method such as FISH. However, in many cases, genomic gains or losses only partially overlap BAC clones on the array, resulting in weak evidence of gain or loss of chromosomal material. These aberrations may not be confirmed using BAC-derived FISH probes, leading to apparent inconsistencies between array and FISH results. Additionally, in cases of very small and large chromosomal imbalances, the size of the alteration can only be estimated based on the size and spacing of the involved probes. High density oligonucleotide arrays can be used to confirm the chromosomal alterations identified by BAC array CGH and can also provide more accurate information regarding aberration size and endpoints.

Design: In the present study, confirmatory high resolution oligonucleotide array CGH (Agilent Tech.) analysis was performed on DNA samples from ten DD-MR cases with diagnostic abnormalities identified by BAC array CGH (Combimatrix Mol. Diag.). Alteration endpoints, aberration size, and involved genes were identified and evaluated.

Results: High resolution oligonucleotide array CGH confirmed the abnormalities identified by BAC array CGH in ten of ten cases (for example, see Figure). Approximate alteration endpoints were noted and gene lists from these regions were generated.

Conclusions: High resolution oligonucleotide array CGH is a sensitive, reliable and effective method for confirmation of abnormal BAC array CGH results.

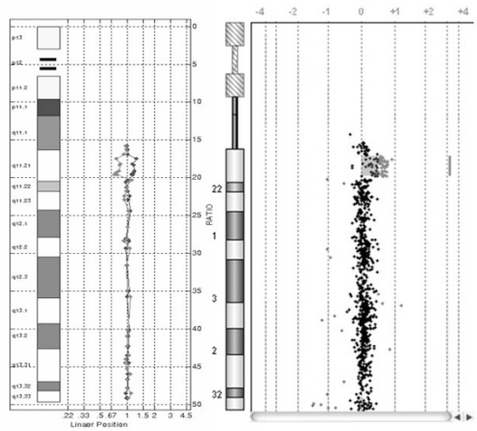

22q duplication identified by BAC array CGH.

2.4 Mb 22q duplication confirmed by oligonucleotide array CGH.

1664 Remote "Glass-Less" Gastrointestinal Pathology Consultation Via Virtual Microscopy

S Jakate, D Giusto, K Bloom. Rush University Medical Center, Chicago, IL; Clarient Diagnostic Services, Aliso Viejo, CA.

Background: Advances in high-resolution digital image technology have enabled optimal simulation of conventional histological evaluation of glass slides and the ability to remotely perform consultation securely through a web-browser and suitable software. We describe our recent experience of 101 such virtual microscopy gastrointestinal pathology consultation cases where concurrent or "back-up" glass slides were never examined. We also assess the ramifications of such consultation in all aspects of client services.

Design: Primary pathologists from several US states send their cases for immunohistochemical staining as well as expert histological opinion to an advanced laboratory ("secondary pathologist"). Between August 2006 and September 2007 (13 months), the secondary pathologist sought tertiary consultation on 101 GI cases by paper-less patient information and glass-less virtual microscopy. All client service aspects comparable to conventional consultation, such as case notification, patient registration and clinical information, image review and recording, report delivery and turn-around-time were assessed.

Results: Tertiary consultant was alerted of registered virtual cases by simultaneous text-page and e-mail and could immediately access the case via secure log-on to the secondary pathologist's site on the web. Scanned documents pertaining to patient registration data, primary pathologist s preliminary report, and pertinent clinical information such as endoscopic and/or imaging reports were available in all cases. All scanned slides could be viewed through special software and the images easily downloaded. The tertiary consultant re-registered the case in his own IS, evaluated the clinical data and slides, generated a report with images, created a PDF report and securely e-mailed the report to the secondary pathologist in total of less than 20 minutes in 95% cases. In 5% cases there was a delay for clinical information or immunostaining. The primary or secondary pathologists or submitting physicians have not identified any diagnostic or patient information errors by the tertiary pathologist in any case.

Conclusions: Virtual microscopy is a highly efficient and secure avenue for subspecialty consultation that obviates the need for paper-work and glass-slide review. All aspects of conventional evaluation are substituted and the entire process is far speedier while at the same time providing the consultant with the ease of image capture and flexibility of work hours and work-place.

1665 Molecular Surgical Pathology: Detection of Various c-kit Mutations in GISTs from the Formalin-Fixed Paraffin Embedded (FFPE) Sections for Molecular Targeted Cancer Therapy

H Kajiya, H Kajiwara, A Serizawa, H Ito, S Takekoshi, RY Osamura. Tokai University School of Medicine, Isehara, Kanagawa, Japan.

Background: It has been well known that c-kit mutations in the gastrointestinal stromal tumors (GISTs) are associated with the responsiveness to Imatinib therapy. Frequently, in our practice, the available tissues are limited to archival FFPE materials. This study is to elucidate the feasibility of FFPE to detect various c-kit mutations such as deletion, insertion and point mutation.

Design: 4μm sections from the archival FFPE blocks of GISTs (2000-2005) were subjected to the following mutation studies. The targeted areas were microdissected and DNA was extracted using proteinase K and phenol + chloroform solution. Polymerase chain reaction (PCR) for c-kit exon9 and exon11 were carried out using Amplitaq Gold (Applied Biosystems) according to the manifacture's instruction. Mutations were analyzed from the amplified DNA by direct DNA sequencing. Immunohistochemical staining for c-kit (Novocastra) was performed with the Envision system (DAKO). Autoclave heating was done for the antigen retrieval.
Results: Among the gastric GISTs, two cases showed point mutation (CTT→CCT in codon1803: Leu^{576}→Pro), one case revealed deletion mutation (27bp deletion: codon 1724~1750), both in Exon 11. One case showed the absence of mutation. A case of the duodenal GIST had insertion mutation (insertion:codon 1585-1586 Tyr^{503}-Ala-Tyr-Phe^{504}) in Exon 9. In the duodenal GIST, both spindle cell and epithelioid areas showed the same mutation. No correlation was noted between mutations and IHC staining in these GISTs.
Conclusions: With the appropriate design of primers, various mutations in c-kit gene, i.e. deletion, insertion, point mutations in Exons 9 and 11 can be detected from the FFPE sections. Our studies recommend the performance of mutation study from FFPE to be included in surgical pathology practice for appropriate patient care.

Sense and antisense sequencing of c-kit exon9 and 11

Exon 9F	5' ATGCTCTGCTTCTGTACTGCC 3'
Exon 9B	5' CAGAGCCTAAACATCCCCTTA 3'
Exon 11F	5' CCAGAGTGCTCTAATGACTG 3'
Exon11B	5' ACCCAAAAAGGTGACATGGA 3'

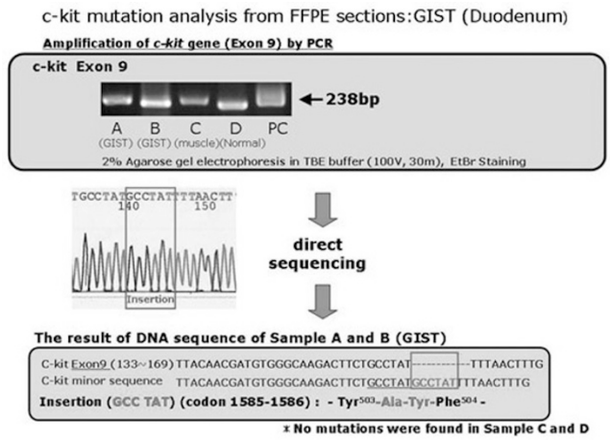

1666 Tissue Microarray Core Dissection Opens Pathology Archives for Expression Array Analysis

C LaFargue, S Perner, S Setlur, Y Hoshida, F Demichelis, MA Rubin. Brigham and Women's Hospital, Boston, MA; Broad Institute of MIT and Harvard, Cambridge, MA.

Background: Protocols facilitating expression profiling studies on formalin fixed paraffin embedded (FFPE) samples are imperative to open pathology archives for large-scale studies with long-term outcome. We developed a tissue microarray (TMA) core dissection protocol allowing for high sampling accuracy and RNA yield.
Design: To assess tissue core homogeneity, 18 equally distributed sections taken from a standard TMA with 432 tissue cores were analyzed. To assess RNA yield, three biopsy cores (0.6 mm diameter) were dissected from 20 tumor samples for targeted tissue sampling and RNA extraction. These cores were taken from regions containing <10% non-target tissue contamination. 11 samples were interrogated using the Illumina DASL (cDNA-mediated annealing, selection, extension, and ligation assay) platform to compare expression profiles from standard serial tissue sectioning versus the coring approach.
Results: In 97.3% (397/408) of the cores, the initial target diagnosis remained the same throughout the depth (Z-axis) of the core. Hence, the cores were homogeneous allowing isolation of pure target tissue. Three cores per sample yielded sufficient RNA (400ng) for the DASL platform. In 65% of cases, one core was sufficient to obtain enough RNA. Comparison of expression of individual genes using matched core and standard sectioning from 11 samples showed a strong correlation for normalized expression levels of ~6000 interrogated genes ($R^2 = 0.93$). Unsupervised hierarchical clustering analysis revealed that the core and standard tissue section pair from each sample clustered together.
Conclusions: Our novel, highly target-specific tissue-preserving protocol allows for RNA extraction in a time-efficient manner facilitating large-scale gene expression studies using the Illumina DASL platform.

1667 Consistent IHC HER2 Image Analysis on ScanScope Systems

H Lange. Aperio Technologies Inc., Vista, CA.

Background: Reliable image analysis requires consistent slide scanning. Aperio's ScanScope systems provide an automatic calibration each time a slide is scanned that compensates for the current light and optical variations; superior to factory or daily calibration. Aperio's IHC HER2 Image Analysis (IA) algorithm provides the HER2 score and the percentages of 1+, 2+ and 3+ cells allowing measuring any system variations with high precision. A suite of reproducibility studies were conducted to measure the variations introduced by the systems, operators and pathologists.
Design: The same 8 HER2 slides with 2 slides per HER2 score 0, 1+, 2+ and 3+ were used for all studies. The slides were scanned 20 times on the same ScanScope system (S1) on different days (#1), and 10 times on 3 different ScanScope systems (S1, S2, S3) on the same day (#2). Different operators scanned the slides for the different runs. The same regions for analysis were used over all runs to eliminate the variations introduced by the pathologists. The slides were annotated with the regions for the analysis 5 times by the same pathologist (#3), and once by three different pathologists (#4). The same digital slides (no rescanning) were used to eliminate the variations introduced by the system. The HER2 score agreement and overall average standard deviation (SD) and range (max – min) for the cumulative percentages of 1+, 2+ and 3+ cells (0-100%) were evaluated.
Results: The IHC HER2 IA results show for all intra- and inter-system runs a perfect HER2 score agreement (100%) and a very consistent very small average SD and range with 0.67% SD 1.68% Range for #1, 0.69% SD 1.22% Range for #2-1, 0.73% SD 1.28% Range for #2-2, 0.70% SD 1.28% Range for #2-3 and 0.78% SD 1.93% Range for #2-1, 2, 3 combined. No inter-operator variability was observed. The IHC HER2 IA results for the intra-pathologist and inter-pathogists runs show significant lower HER2 score agreements and less consistent and larger average SD and range with 90% HER2 score agreement 2.44% SD 3.51% Range for #3 and 83% HER2 score agreement 9.77% SD 11.20% Range for #4. As comparison we would expect a significant lower overall HER2 score percent agreement of about 75% for inter-pathologists performance using manual microscopy.
Conclusions: Aperio's ScanScope systems provide excellent reproducibility from scan to scan and from instrument to instrument. System variations are insignificant compared to the variations introduced by the pathologists due to choosing the regions for analysis.

1668 Separation of Invasive Lobular from Ductal Carcinoma of the Breast Using Raman Molecular Imaging

JL Lindner, S Stewart, J Maier, J Cohen, JF Silverman. Allegheny General Hospital, Pittsburgh, PA; ChemImage, Corp., Pittsburgh, PA.

Background: Distinguishing invasive ductal carcinoma (IDC) from invasive lobular carcinoma (ILC) can occasionally be difficult. E-cadherin immunohistochemical (IHC) staining is helpful in distinguishing between these two carcinomas. Raman Molecular Imaging (RMI) is an analytical tool employed in many industrial applications due to its high molecular specificity and reagentless capability. Based on the interaction of light with molecules, RMI yields the image of a sample wherein each pixel in the image corresponds to molecular information at that location. With a spatial resolution of approximately 250 nm, RMI provides information based on molecular composition and morphology. We investigated the novel application of RMI for the identification of IDC and ILC, especially in cases that are difficult to diagnose without the employment of E-cadherin IHC staining.
Design: RMI were generated from unstained sections of tissue. Ten cases were analyzed and consisted of 3 histologically definitive IDC and 3 ILC, and 2 IDC and 2 ILC that needed E-cadherin IHC staining for a more definitive classification. Measurements derived from RMI of these tissue samples were analyzed using chemometric techniques established in analytical spectroscopy. Chemometrics is a class of mathematical techniques employed to reduce large data sets, to smaller ones acquired in RMI. One chemometric technique is Mahalanobis distance analysis (MD), which measures similarity between classes.
Results: MD was employed by specifying IDC and ILC cases as two different classes. Forty fields of view (FOV) of IDC and 28 FOV of ILC were evaluated in this preliminary investigation. MD yielded results indicating definitive distinction between IDC and ILC data. Evaluation of the principle component scores in the model, using a two-sample z-test, yielded a p value of < 0.01, confirming significant differences between the 10 cases of IDC and ILC, including the 4 indeterminate cases based on conventional H&E examination.
Conclusions: Preliminary results indicate that RMI can distinguish between IDC and ILC, based on the chemical and molecular profile. Therefore, RMI may be a new analytical technique that can potentially assist pathologists in better classifying invasive breast carcinomas that have overlapping or indeterminate pathology, requiring additional ancillary studies.

1669 Combined Fluorescence In Situ Hybridization (FISH) for Telomeres and Centromeres Provides Rapid and Simple Discrimination of Species of Origin for Cells in Tissue Recombination Experiments

AK Meeker, D Vander Griend, Y Konishi, JT Isaacs. Johns Hopkins University School of Medicine, Baltimore, MD.

Background: Tissue recombination followed by implantation into an immuno-compromised murine host represents a powerful method for addressing fundamental questions regarding organogenesis and, when genetically altered cells are used, disease processes. Likewise, in the cancer field, human xenografts have proven very useful. However, in some instances, such as when working with minute material, or when combining cells from more than one species, it can be difficult to discern the implanted cells from those of the host or other admixed cells. Here we present a simple, rapid and robust method for discriminating species of origin for cells implanted in nude mice.
Design: Formalin-fixed paraffin-embedded samples were made from tissue recombinants in which urogenital sinus mesenchyme (UGSM) was isolated from E17 Sprague-Dawley rat embryos, and combined with non-tumor human prostate spheres which had been isolated from a radical prostatectomy specimen. Implants were embedded in Type I collagen, incubated in PrEGM (Lonza) containing 1nM R1881 for 48 hours, and implanted under the renal capsule of male athymic *nu/nu* mice (Harlan Sprague-Dawley, Indianapolis, IN). After 14 and 21 days of growth the implants were excised

and fixed for analysis. Tissue samples were likewise obtained from human tumor xenografts growing in nude mice. 5 micron tissue sections were processed for FISH using a Cy3-labeled hybridization probe that recognizes all mammalian telomeres and a FITC-labeled probe recognizing human and nu/nu mouse centromeres, but not Sprague-Dawley rat centromeres.
Results: Human tumor xenograft cells were easily distinguished from host murine cells by the dramatic differences in telomere lengths between the two species. Likewise, cells were easily differentiated in the tissue recombinants despite the presence of 3 different species. Human cells had bright centromere signals and dim telomere signals while rat cells had the opposite phenotype. Mouse cells were easily identified by strong staining reaction with both probes.
Conclusions: Combined telomere and centromere FISH represent a simple, rapid and robust method for identifying human xenograft cells and species of origin for tissue recombinants growing in nude mice.

1670 Tissue Banking and Pathology Tool Work Space of Cancer Biomedical Informatics Grid – A Model-Driven and Standard Based Informatics Framework To Expedite Translational Research

SK Mohanty, AT Mistry, RS Crowley, M Watson, R Nagarajan, W Amin, AV Parwani, AK Pople, L Schmandt, R Dhir, MJ Becich. University of Massachusetts School of Medicine, Worcester, MA; University of Pittsburgh School of Medicine, Pittsburgh, PA; Washington University School of Medicine, St. Louis, MO.
Background: Biospecimens are incredible resources to accelerate the growing requirements of the oncology research community facilitating translational research studies. As a result, the modern molecular medicine is driving demand for high-quality biospecimens for translational research to support clinical trials, biomarker validation studies, and the development of targets for innovative therapeutic options. The National Cancer Institute's Cancer Biomedical Informatics Grid (caBIG™) initiative was launched to address the aforementioned objectives. To accomplish this goal, the Tissue Banking and Pathology Tools (TBPT) Workspace was developed within the grid domain. Here we discuss the various components of the TBPT Workspace along with their development and deployment within the grid.
Design: The components of TBPT Workspace include cancer Text Information Extraction System (caTIES), caTISSUE Clinical Annotation Engine (CAE) and caTISSUE Core. These tools were based upon a set of Common Data Elements with controlled vocabulary and ontology to offer semantic and syntactic interoperability.
Results: The TBPT Workspace tools have been developed by the University of Pittsburgh, (caTIES and caTISSUE CAE) and Washington University (caTISSUE Core).The caTIES is an very efficient tool to extract information from the free text fields of archival surgical pathology report. The caTISSUE Core is an enterprise tissue bank. The CAE is a proficient tool for annotation of biospecimens integrating structured data from clinical, pathology, and molcular systems. These systems altogether work in integration to provide high-quality biospecimens.
Conclusions: The caBIG is an enterprise bioinformatics platform that facilitate cancer research by connecting organizations, institutions and individuals. It enables sharing of data, infrastructure and tools. Ultimately this will evolve into a self-sustaining community that encompasses the global translational research.

1671 Rapid *In Situ* Hybridization for Fungal Pathogens Using a Peptide Nucleic Acid (PNA) Probe Targeting a Panfungal rRNA Sequence

KT Montone. University of Pennsylvania Medical Center, Philadelphia, PA.
Background: Peptide nucleic acids (PNA) are artificially constructed nucleotides similar to DNA and RNA. PNA backbone is composed of repeating N-(2-aminoethyl)-glycine units linked by peptide bonds and PNAs act more like peptides. PNA probes have advantages over DNA oligonucleotide probes: binding between PNA/DNA is stronger than DNA/DNA, PNAs are not easily recognized by nucleases or proteases and PNAs are stable over a wide range of pHs. Therefore, they make great tools for *in situ* hybridization (ISH). Because of the peptide background, PNA probes are believed to have enhanced tissue permeability and may be useful tools for detecting rRNA sequences of infectious agents. PNA probes have not been widely utilized for detecting fungal pathogens in paraffin-embedded tissues. In this study, a PNA oliognucleotide probe against a panfungal rRNA sequence was used in an attempt to develop an assays for detecting fungi by PNA ISH.
Design: A panfungal specific PNA probe with the following sequence 5'-GGACGTGCCCGAAATGGA-3' was commercially synthesized and 3' biotin labeled. ISH was performed on formalin fixed, paraffin-embedded tissue samples demonstrating a variety of fungal infections including *Aspergillus sp*, *Candida sp*., *C. neoformans*, *H. capsulatum*, *S. schenkii*, *B. dermatitidis* as well as single cases of *Ochroconis gallopava* and *Scedosporium apiospermum*. ISH was performed using manual capillary action technology on the Microprobe staining system. The tissues were rapidly dewaxed, cleared, rehydrated and then digested with 2.5 mg/ml of pepsin. The PNA panfungal probe was applied at a concentration of 2 ng/ul to the tissue sections and heated at 105°C briefly followed by hybridization for 1 hour at 55°C. Following 3, 5 minute washes in 2XSSC at 55°C, the hybrids were detected using either anti-biotin conjugated to alkaline phosphatase or anti-biotin conjugated to horse-radish peroxidase with Permanent Red or AEC as the chromogen respectively. The procedure time was approximately 2.5 hours.
Results: The ISH procedure detected fungal pathogens in all of the specimens examined. Most of the fungal organisms stained with the procedure with the exception of *C. neoformans* in which <50% of the organisms stained with the assay.
Conclusions: ISH with PNA probes can be utilized to identify fungal pathogens in formalin-fixed, paraffin-embedded tissues. These methods may be useful to rapidly identify fungal pathogens when cultures are not performed or when a fungal pathogen is observed and cultures are negative.

1672 Reading Digital IHC Slides on a Computer Monitor – A Multi-Site Performance Study Using 180 HER2 Stained Breast Specimens

A Nassar, C Cohen, MT Siddiqui, M Albitar, SS Agersborg, W Zhou, KA Lynch, ER Heyman, AH Olson, H Lange. Mayo Clinic, Rochester, MN; Emory University Hospital, Atlanta, GA; Quest Diagnostics Nichols Institute, San Juan Capistrano, CA; Aperio Technologies Inc., Vista, CA.
Background: With the adoption of digital pathology, image analysis of immunohistochemistry (IHC) slides can be integrated seamlessly into the digital pathology workflow. A pathologist can now use image analysis efficiently while reading the digital IHC slides on a computer monitor. Thus, the clinical acceptance of a digital pathology system for IHC quantitation depends both on the performance of the IHC image analysis, and the ability of manually reading digital IHC slides on the monitor. A multi-site study was conducted to compare the manual reading of digital IHC Human Epidermal growth factor Receptor 2 (HER2) slides on a monitor, using Aperio Technologies, Inc.'s ScanScope® XT instrument and Spectrum™ digital pathology information management system to conventional manual microscopy.
Design: 180 breast cancers were immunohistochemically stained using Dako's HercepTest™ were assayed; (site 1) 80 routine specimens from EUH, and (site 2) 100 specimens with equal HER2 score distribution from Quest. At each site, three pathologists performed a blinded read of the glass slides using a conventional light microscope, and reporting the HER2 score for each. The glass slides were scanned using a 20X objective, and after a wash-out period and randomization of the slides, the same three pathologists performed another blinded read of the same slides, but this time of the digital image on the monitor, again reporting the HER2 score. Each of the methods: manual microscopy and manually reading digital IHC HER2 slides on a monitor were evaluated separately and comparatively using Percent Agreement (PA) of negative HER2 scores (0, 1+) vs. positive HER2 scores (2+, 3+).
Results: Comparable PA values were obtained for manual microscopy (MM) and for manually reading digital (DR) IHC HER2 images on the monitor (MM: 77.5% - 93.8% site 1, 89.0% - 92.0% site 2 / DR: 80.0% - 88.8% site 1, 82.0% - 89.0% site 2; DR vs. MM: 75.0% - 96.3% site 1, 88.0% - 93.0% site 2).
Conclusions: Results of manually reading digital IHC HER2 images on a monitor using Aperio Technologies, Inc.'s digital pathology system show substantial equivalence to those obtained by conventional manual microscopy. The large images on the monitor are easy to read.

1673 Trainable IHC HER2 Image Analysis System for Dako's HercepTest and Ventana's PATHWAY HER2 – A Multi-Site Performance Study Using 260 Breast Tissue Specimens

A Nassar, MT Siddiqui, C Cohen, SS Agersborg, W Zhou, KA Lynch, M Albitar, BL Vanderbilt, EA Barker, H Lange, J Thompson, ER Heyman, A Olson. Mayo Clinic, Rochester, MN; Emory University Hospital (EUH), Atlanta, GA; Quest Diagnostics Nichols Institute, San Juan Capistrano, CA; Medical Laboratory Associates (MLA), Seattle, WA; Aperio Technologies Inc., Vista, CA.
Background: Clinical laboratories have a choice between different reagents for their Immunohistochemistry (IHC) Human Epidermal growth factor Receptor 2 (HER2) staining. Aperio provides a new IHC HER2 Image Analysis (IA) system that allows tuning the intensity thresholds of the HER2 scoring scheme to adapt to the staining characteristics of different reagents. Automated training provides the optimum intensity thresholds based on a set of representative slides that have been scored by qualified pathologists. A multi-site study was conducted comparing the trainable IHC HER2 IA system results for different reagents to those by manual microscopy (MM).
Design: 260 formalin-fixed, paraffin-embedded breast tissue specimens from 3 clinical sites were assayed; 80 specimens with equal HER2 score distribution from EUH and 100 routine specimens from Quest all stained with Dako's HercepTest, and 80 specimens with equal HER2 score distribution from MLA stained with Ventana's PATHWAY® HER2. At each site, 20 representative slides with scores from 3 pathologists were used to automatically train the IHC HER2 IA system. At each site, 3 pathologists performed a blinded read of the glass slides using a microscope. The glass slides were scanned and after a wash-out period and randomization, the same 3 pathologists outlined a representative set of tumor regions to be analyzed by IHC HER2 IA. The algorithm itself was run in batch mode. Each of the methods: MM and IA were evaluated separately and comparatively using Percent Agreement (PA) of negative HER2 scores (0, 1+) vs. positive HER2 scores (2+, 3+).
Results: Comparable PA values for IA and MM of the two differentially stained slide sets were obtained across all sites: MM: 77.5–93.8%, IA: 95-97.5%, MM vs. IA: 83.8-95% for EUH; MM: 89–92%, IA: 87-96%, MM vs. IA: 85-94% for Quest; MM: 71.3–85, IA: 93.8-96.3%, MM vs. IA: 73.8-83.8 for MLA.
Conclusions: Aperio's trainable IHC HER2 IA system not only shows substantial equivalence to MM for Dako's HercepTest™ and Ventana's PATHWAY® HER2, but also improves concordance.

1674 Estrogen Receptor Immunohistochemistry for Confirmation of Sentinel Lymph Node Metastasis in Cases with Equivocal Cytokeratin Positivity

CV Nguyen, MT Deavers, J Quinones, L Huo. M.D. Anderson Cancer Center, Houston, TX.
Background: Immunohistochemical staining for cytokeratin (CK) is commonly used in the evaluation of sentinel lymph nodes (SLNs) for occult breast carcinoma metastases. In some cases the nature of CK(+) cells is not clear, and differentiation of true metastases from non-epithelial cells can be problematic. The purpose of this study was the evaluation of estrogen receptor (ER) immunostaining superimposed on CK, as a method for the confirmation of metastasis when CK immunostaining alone is equivocal.
Design: From our files, we found 3 cases of SLNs in which CK(+) cells were equivocal for malignancy. The primary tumor in each case (1 invasive ductal [IDC],

1 invasive lobular [ILC], and 1 invasive mammary carcinoma with ductal and lobular features [IMC]) was known to express ER (90%, 100%, and 50%, respectively). Immunohistochemical staining using an antibody against ER (red chromogen, nuclear staining) was performed on the same slides that had been stained for CK (DAB, cytoplasmic staining). In addition, 3 known positive and 4 known negative SLNs (all from patients whose primary tumors had 90% or more ER expression) served as control groups and were stained with the same technique. The results of staining for ER superimposed on CK in the three equivocal cases were compared with the controls.

Results: Two of three positive controls had CK(+) cells that stained strongly for ER (>80% cells). The third positive control (which contained only 3 CK(+) cells) did not stain for ER. In all 4 negative controls, non-epithelial cells with CK staining were negative for ER. In the equivocal cases, the IDC case originally had a cluster of smudgy cells (0.08 mm) in the subcapsular sinus that had much weaker CK positivity when compared to the primary tumor. All the cells in the cluster stained strongly for ER in this case. The ILC case originally had 6 cells with inconclusive CK staining. ER stained 2 of the 6 cells. Finally, the IMC case originally had a small area of CK(+) cells (<1.0 mm) that was indefinite for tumor cells. ER strongly stained all of the CK(+) cells. Occasional lymphocytes in most of the cases also stained for ER.

Conclusions: ER immunohistochemical staining superimposed on CK in SLNs can be useful in cases when CK staining alone is equivocal, particularly when the primary tumor is known to have high expression of ER. A positive ER stain superimposed on CK helps to confirm metastasis. In contrast, a negative ER stain does not exclude metastatic disease.

1675 Image Cytometric Validation of Breast Carcinoma Markers Using Tissue Microarrays: Rabbit Monoclonal Versus FDA-Approved Antibodies

CM Norton, C Cohen, D Lawson, A Nassar. Emory University, Atlanta, GA; Mayo Clinic, Rochester, MN.

Background: Immunohistochemistry (IHC) provides diagnostic information and predicts response to targeted therapies. It lacks reproducibility due to poor standardization and subjective interpretation. Automated image cytometric systems are available to improve accuracy in result interpretation. In addition, rabbit monoclonal antibodies (RMab) may be a source of higher sensitivity. This study uses the ACIS III (Dako) with tissue microarrays (TMAs) to compare RMab to ER, PR, Her2, and MIB-1 with FDA-approved antibodies (FMab).

Design: TMAs of 43 breast cancers were used. IHC was performed using RMab (LabVision): ER (SP1; 1/100), PR (SP2; 1/400), Her2 (SP3; 1/100), MIB-1 (SP6; 1/200). FMab (Dako) used: ER (1D5; 1/50), PR (PgR636; 1/400), Herceptin kit, MIB-1 (Mib-1; 1/160). The stained TMAs were quantitated visually and by image cytometry (ACIS III). Less than 5% was negative for ER and PR. Visual Her2 3+ >30% was positive, 3+ </= 30% and 2+ >/= 10% equivocal, 0 and 1+ negative. Her2 image analysis: <1.8 negative, 1.8-2.2 equivocal, >2.2 positive. MIB-1 was low (<10%), intermediate (10-20%), and high (>20%).

Results:

	Pos agreement %	Neg agreement %	Kappa	P value
ER VRMab vs VFMab	100	87	0.8	0.1
ER IRMab vs IFMab	100	93	0.9	0.3
ER VRMab vs IRMab	100	100	1	1
ER VFMab vs IFMab	96	100	0.9	0.3
PR VRMab vs VFMab	100	0	0	0.0005
PR IRMab vs IFMab	100	0	0	0.0016
PR VRMab vs IRMab	100	-	-	-
PR VFMab vs IFMab	100	100	1	1
Her2 VRMab vs VFMab	40	96	0.5	0.01
Her2 IRMab vs IFMab	73	100	0.9	0.2
Her2 VRMab vs IRMab	89	100	0.9	0.3
Her2 VFMab vs IFMab	91	90	0.9	0.7

	Low agreement %	Intermediate agreement %	High agreement%	Kappa	P value
MIB VRMab vs VFMab	50	69	82	0.7	0.08
MIB IRMab vs IFMab	36	50	50	0.4	0.04
MIB VRMab vs IRMab	100	80	87	0.9	0.3
MIB VFMab vs IFMab	100	67	73	0.9	0.11

V=visual I=image analysis.

Conclusions: There was excellent agreement between RMab vs FMab in TMA for ER and PR expression by both visual and image analysis. Her2 expression was in fair-excellent agreement between the two antibodies, excellent by both assays. For MIB-1, there was fair-moderate concordance between both antibodies, excellent by both methods.

1676 Immunohistochemical (IHC) Detection of DNA Mismatch Repair (MMR) Proteins in Sebaceous Neoplasms: Patterns and Clinical Significance

L Orta, K Busam, P Mecca, L Tang, D Klimstra, J Shia. Memorial Sloan-Kettering Cancer Center, NY.

Background: IHC detection of DNA MMR proteins in colorectal carcinoma has emerged as a useful screening tool for identification of patients at risk for hereditary nonpolyposis colorectal cancer (HNPCC). Muir-Torre syndrome (MTS) is a variant of HNPCC characterized by sebaceous neoplasms and visceral malignancy. The utility of IHC in sebaceous tumors for identifying MTS has not been well studied.

Design: We identified 21 patients with ≥ 1 extra-ocular sebaceous carcinoma (SC), 4 with ≥1 sebaceous adenoma (SA), 4 with SCs and SAs, and 8 with sebaceous hyperplasia (SH). IHC staining for MLH1, MSH2, MSH6 and PMS2 was analyzed, and correlated with patients' clinical findings.

Results: IHC staining was interpretable in all samples. As listed in Table 1, no SH showed IHC abnormalities, but 9 of 25 (36%) patients with SC and 7 of 8 (88%) with SA showed loss of staining for at least 1 protein. The patterns of abnormality were identical in SCs versus SAs in the same patients; the most common being concurrent loss of MSH2 and MSH6. Comparing to IHC-normal group, IHC-abnormal patients tended to be younger, and more likely to have HNPCC-related visceral malignancies and a family history fulfilling the Amsterdam criteria (AC) for HNPCC or Bethesda Guidelines (BG) for testing tumors for microsatellite instability (Table 2).

Table 1. Number of patients or samples showing various IHC staining patterns.

		IHC Normal	IHC Abnormal				
			Loss of PMS2 alone	Loss of MSH6 alone	Loss of MLH1/PMS2	Loss of MSH2/MSH6	Total
SC	Samples (n=35)	19	1	0	1	**14**	16
SC	Patients (n=25)	16	1	0	1	**7**	9 (36%)
SA	Samples (n=14)	2	1	1	2	**8**	12
SA	Patients (n=8)	1	1	1	2	**3**	7 (88%)
SH	Samples (n=9)	9	0	0	0	**0**	0
SH	Patients (n=8)	8	0	0	0	**0**	0

Table 2. Correlation between IHC results of sebaceous neoplasms and patients' clinical characteristics.

IHC	Median age (years); Male:female ratio	Visceral malignancies	Family history				
			Positive*	BG	AC	None	Not available
Normal (n=17)	69; 6:11	12 with none; **1 with HNPCC-related tumor**; 4 with non-HNPCC-related tumor.	4	**2**	**0**	3	8
Abnormal (n=12)	56.5; 8:4	3 with none; **7 with HNPCC-related tumor**; 2 with non-HNPCC-related tumor.	1	**2**	**5**	3	1

*Not fulfilling BG or AC.

Conclusions: IHC detection of MMR proteins in sebaceous tumors is feasible. IHC abnormality in SC and/or SA correlates with the presence of visceral malignancy and positive family history, demonstrating the utility of IHC in sebaceous tumors to identify patients at risk for genetic defects in DNA MMR.

1677 Intraoperative Frozen Section Fixation with Formalin Improves Diagnostic Accuracy of Tumors with Clear Cells, Papillary Architecture, or Micropapillary Type Invasion

K Patel, Z Schreiber, PB Kane, S Liang, J Liu, C Tornos. Stony Brook University Medical Center, Stony Brook, NY.

Background: Some of the histologic features used to diagnose certain tumors are better observed on permanent sections following formalin fixation, namely clear cells, papillary architecture, micropapillary type of invasion, and nuclear clearing of thyroid papillary carcinoma. The aim of the study is to compare intraoperative diagnostic accuracy of frozen sections (FS) fixed with either ethanol or formalin in cases with such features.

Design: Two FS of 10 ovarian/peritoneal serous carcinomas, 5 papillary thyroid carcinomas, 3 renal cell carcinomas conventional/clear cell type, and 3 clear cell ovarian carcinomas were cut and then fixed for 10 seconds one with ethanol and one with formalin. Both slides were then stained using the same hematoxylin and eosin technique commonly used in the FS laboratory. The cases were then reviewed by 2 of the authors.

Results: Eight of the ten ovarian serous carcinomas showed a predominant solid pattern on the slide fixed with ethanol. On the slide fixed with formalin, six of these eight cases showed an obvious papillary architecture, and the remaining two showed micropapillary type of invasion. The FS fixed in ethanol from the 3 renal cell carcinomas and the 3 clear cell carcinomas showed a predominance of eosinophilic cells and a solid architecture. The FS fixed in formalin of all six cases showed a predominance of clear cells. In addition, in two of the clear cell ovarian tumors, the formalin-fixed FS showed partial papillary areas. In contrast, all 5 thyroid carcinomas fixed in ethanol showed better cytologic nuclear detail characteristic of papillary carcinomas including grooves, irregular contour, and pseudoinclusions. Nuclear clearing (Orphan-Annie nuclei) was not seen with either fixation.

Conclusions: Intraoperative frozen section fixation with formalin enhances the papillary architecture of ovarian serous and clear cell carcinomas, as well as micropapillary type of invasion in serous carcinomas. Formalin fixation also augments the clear cell appearance of renal cell carcinomas and ovarian clear cell carcinomas. This enhancement facilitates the accurate diagnosis of these lesions. Diagnostic features of papillary thyroid carcinoma are demonstrated best in FS after ethanol fixation.

1678 Use of a Novel FISH Assay as an Adjunct to Diagnosis of Dermatofibrosarcoma Protuberans and Giant Cell Fibroblastoma

HR Peck, M Nelson, F Pedeutour, Z Gatalica, M Miettinen, JA Bridge. U Nebraska Med Ctr, Omaha, NE; Hospitalier Universitaire, Nice, France; Creighton Med Ctr, Omaha, NE; Armed Forces Inst of Pathology, Washington, DC.

Background: DFSP and GCF are characterized by a *COL1A1/PDGFB* fusion [t(17;22)(q22;q13)]. Identification of this characteristic fusion may be diagnostically useful when confronted with DFSP/GCF lesions arising in uncommon sites, deviating from the classic histologic appearance, or exhibiting fibrosarcomatous transformation. As a diagnostic aid, we constructed FISH probe sets that: 1) can be performed on paraffin-embedded, formalin-fixed tissue; 2) identify potential unusual variant translocations or cryptic rearrangements; and 3) assess individual histologic components such as fibrosarcoma arising in DFSP.

Design: Probe cocktails of selected BAC/PAC clones were developed to assess *COL1A1* and *PDGFB* loci independently or as a fused translocation event. After establishing the specificity of the probes [on established 17;22 rearranged DFSP metaphase cells and normal lymphocytes], we evaluated metaphase cells, touch preparations or paraffin-embedded tissue sections of 26 specimens [16 DFSPs including an unusual case arising in the uterus and another exhibiting a variant 2;17 translocation, 2 DFSPs with fibrosarcomatous transformation, 3 GCFs, 2 dermatofibromas (DFs) and 3 pathologically unremarkable skin specimens] using two-color FISH assays.
Results: *COL1A1/PDGFB* fusions were detected by FISH in 14 of 16 DFSPs including the uterine DFSP and the t(2;17) characterized DFSP (cryptic 17;22 rearrangement), both fibrosarcomatous DFSPs and all GCFs. The FISH findings were concordant in the 6 DFSPs that also had informative results for RT-PCR or conventional karyotyping. One DFSP did not show *COL1A1* or *PDGFB* rearrangements or a *COL1A1/PDGFB* fusion. Another DFSP was not successfully analyzed; possibly due to prolonged formalin fixation. Gains of *COL1A1/PDGFB* genomic copies were not detected in the fibrosarcomatous areas when compared to the DFSP areas in the 2 fibrosarcomatous DFSPs. *COL1A1/PDGFB* fusions were absent in the DFs and normal skin specimens.
Conclusions: FISH analysis with these newly designed probe sets is a reliable and specific method of detecting t(17;22) in routinely processed tissue (including paraffin-embedded, formalin-fixed tissue) and it may serve as a useful diagnostic aid in DFSP/GCF cases with unusual clinicohistopathologic or fibrosarcomatous features. Moreover, these probe sets are capable of revealing cryptic or variant translocations.

1679 Enhancing the Malignant Cell Population in Culture Chemo-Response Testing

TC Pereira, LM Hancher, JE Bush, SL Brower, LK Mahood, AL Backner, JF Silverman. Allegheny General Hospital, Pittsburgh, PA; Precision Therapeutics, Pittsburgh, PA.
Background: In vitro chemo-response testing in human tumor culture is increasingly performed for individualized cancer therapy. Ensuring that the culture will have a predominant malignant population can be challenging, and different culture protocols have been reported. We compared the effect of a control protocol with 3 other experimental protocols in the enrichment of malignant breast cancer cells for chemo-response testing.
Design: Breast carcinoma samples were mechanically disaggregated by mincing into small pieces using scalpels. In the control protocol the minced tissue was immediately seeded into collagen-coated culture flasks. For the experimental protocols, the minced tissue was first enzimatically disaggregated with Collagenase III (750 U/ml) for 6 hours at 37C with agitation, then subjected to differential centrifugation, resulting in 3 different fractions: organoid, single-cell epithelial and stromal. Each fraction was then seeded into collagen-coated culture flasks. The cultures were incubated at 37C under 5% CO_2. Cytospins of each cell suspension culture were prepared and stained with Diff-Quik and Papanicolaou stain. 300 cells were counted in each slide and individually classified as benign or malignant by a cytopathologist, and the percentage of malignant cells was calculated.
Results: A total of 27 cultures were seeded in 8 different carcinoma specimens. The fibroblast protocol was only performed in 3 specimens. The other 3 protocols were performed in all the cases. The control protocol did not produce a viable cell culture in 3 cases, and in 4 of the 5 remaining cases it produced a higher percentage of malignancy compared to the experimental protocols. Among the experimental protocols, the fibroblast fraction performed similar to the epithelial fraction in the 3 cases that it was done. When comparing the 2 protocols that were successfully performed in all the cases (organoid and epithelial protocols), in 5/8 cases the epithelial protocol demonstrated a superior malignant percentage in both Diff-Quik and Papanicolaou stains.
Conclusions: In 3 of 8 cases, the control protocol produced no viable culture. The experimental protocols with collagenase produced viable cultures in all 8 cases, and had also the advantages of increasing cell yield and reducing turn around time. The experimental single-cell epithelial protocol was superior to the organoid in producing a higher percentage of malignant cells to be used in chemo-response testing.

1680 Digital Archives: A Study of Diagnostic Accuracy, with Evaluation of Multiple Morphologic Parameters and Possible Pitfalls

L Petroff, A Manzo, E Brzostowski, S Patil, E Brogi. Memorial Sloan-Kettering Cancer Center, New York, NY.
Background: Use of digital technologies in pathology is increasing, but skepticism remains regarding the feasibility of diagnosis (DX) based on review of digitally scanned slides (DS). At present, no independent data exists on reproducibility of morphologic parameters using DS. Having creation of a virtual archive as ultimate goal, we conducted a detailed evaluation on DS of submitted cases to assess reproducibility of the DX rendered on glass slides (GS) and identify possible pitfalls.
Design: 220 submitted cases from 179 patients with breast carcinoma (119 core biopsies, 73 excisions, 28 mastectomies) were reviewed between July and August 2007 by 6 pathologists. Each pathologist chose representative GS for digital scanning (Aperio ScanScope XT, Aperio Technologies Inc., Vista, CA) at the time of diagnosis. One pathologist (L.P.) reviewed the DS blindly, noting variables such as (micro) invasive carcinoma (type, tubule formation, nuclear grade (NG), size, vascular invasion (LVI)), in-situ carcinoma (type, NG, architecture, necrosis), margin status, calcifications and biopsy changes. For validation purpose, the pathologist noted the same variables on blind review of the index GS and the same variables were also extracted from the diagnostic reports based on GS. Cohen's kappa value was used to calculate agreement between variables.
Results: Of 1830 GS (average 10.2 GS/case, range 1-62), 659 were scanned (average 3.5 DS/case, range 1-20). The study cases included 154 invasive carcinoma (136 ductal, 17 lobular, 1 mammary), 3 microinvasive carcinoma and 161 in-situ carcinoma (139 DCIS, 21 LCIS, 1 mammary). There was very good agreement between DS and GS for LCIS, tubule formation, microinvasion, and invasive carcinoma, although one invasive carcinoma (2 mm) was not detected on DS (DS likely not reviewed). Agreement was good for: DCIS, NG of invasive ductal carcinoma, LVI, biopsy changes, necrosis in DCIS and margins status; and moderate for the following features of DCIS: NG, architecture and associated calcifications. Poor agreement was noted for calcifications associated with invasive carcinoma.
Conclusions: Our results show that selecting 30-40% of glass slides is sufficient to document the morphologic features of a case. We also demonstrate good to very good reproducibility in the interpretation of multiple diagnostic variables on review of digital slides alone, providing proof of principle for the creation of virtual archives.

1681 Histologic Grade Estimation Using Stochastic Geometry Shape Distributions in Breast Carcinoma

S Petushi, J Zhang, D Breen, FU Garcia. Drexel U. College of Medicine, Philadelphia; Drexel U., Philadelphia.
Background: Subjectivity and low reproducibility of histologic grading in breast carcinoma have been for a long time reasons why the prognostic value of grading has been overlooked. The purpose of the current study was to assess the standardization and reproducibility of grading breast carcinoma by using automated computer-based image analysis based on stochastic geometry shape distributions.
Design: H&E stained slides from paraffin blocks used for prognostic markers from 30 invasive ductal carcinoma cases 10 from each grade using the Nottingham grading system were selected. Each case was reviewed by FUG to confirm histologic grade. An image dataset was created using the entire digitized tissue area in all histology slides. We developed a customized hybrid semi-automated segmentation algorithm to cluster the raw image data and reduce the image domain complexity to a binary representation with the foreground representing regions of high density of neoplastic cells. A second algorithm was designed to apply stochastic geometry and texture analysis measurements in segmented images and produce shape distributions, transforming the original color images to histogram-like representations that characterize their distinguishing properties between grades. Computational results were compared against known histologic grade assigned.
Results: Earth Mover's Distance (EMD) histogram comparison technique was used to study possible correlation between the high-dimensional set of shape distributions to the *a priori* known histologic grades. Results indicate an ability to computationally differentiate between the 3 histologic grades in our dataset of breast cancer cases (Fig. 1).

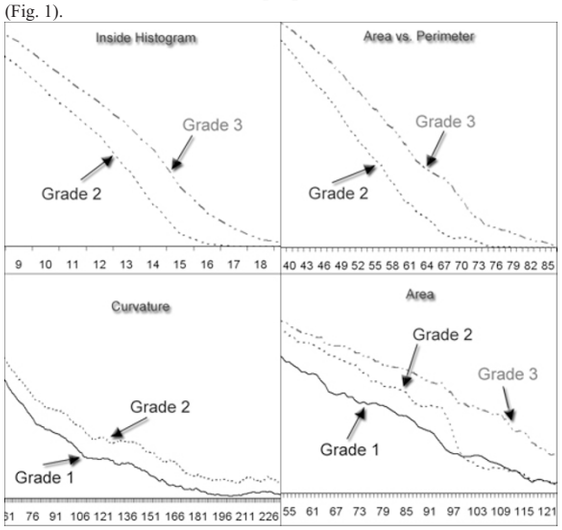

Conclusions: Computational pattern analysis of histologic slides represented as high-dimensional stochastic geometry and texture based shape distributions can be utilized as an effective software tool in breast cancer histologic grading. Incorporating machine learning techniques into a tumor-specific unsupervised clustering framework or semi-supervised classifier would produce a computational algorithmic tool with predictable capabilities making histologic grade more reproducible.

1682 Proliferative Rate Variability and Distribution in Breast Cancer: Implications for Assessment in Tissue Microarrays

DGK Phillips, LG Dressler, J Mackey, D Cowan, M Ellis, OB Ioffe. University of Maryland, Baltimore, MD; University of North Carolina, Chapel Hill, NC; Washington University School of Medicine, St. Louis, MO.
Background: Proliferative rate as measured by MIB-1 (Ki-67) immunohistochemistry is an important prognostic indicator in breast cancer. Since tissue microarrays (TMAs) are widely used to assess tumor profiles, including Ki-67 index, we have set out to assess the degree of intratumoral variability of Ki-67 index in order to determine 1) the distribution of immunostaining within the tumor, and 2) estimate from whole sections the likely contributions that heterogeneity would have on Ki-67 results if the immunostaining was performed on 0.6mm cores (the size of tissue cores in TMAs).
Design: 293 whole sections of invasive breast carcinoma were immunostained with Ki-67 and the staining percentage was determined using the ACIS Chormavision Automated Assisted Image Analysis software. At least 6 and up to 12 measurements were made in

each tumor section, separated from each other by at least 0.6 mm. The location of fields with the lowest and highest indices was recorded, and statistical analysis of labeling variability was performed.

Results: There was significant heterogeneity in the Ki-67 index within tumor sections, similar to the previous reports based on manual estimates. The mean difference between the highest and lowest Ki-67 index was 17.9, and it ranged in individual cases from 0.5 to 83.1 (median 12.1, st. dev 15.8). The standard deviation for each case ranged from 0.9 to 29.8. 154 tumors (52%) had measurements both less and more than 10% (the most commonly used cut-off for Ki-67). 28% tumors showed classic distribution of proliferative rate – highest at the periphery and lowest in the center. 21%of tumors had the reverse labeling distribution. Most commonly, both labeling extremes were present at the periphery of tumor (39%), while in 13% of cases the highest and lowest values were seen in center. With more than 3 observations, the mean percentage was less affected by staining variability.

Conclusions: Although TMAs are highly reliable in mesurement of more homogeneous tumor markers, proliferative rate is highly heterogeneous within many tumors, and TMAs with too few cores per sample could erroneously place a tumor in the wrong risk category. We recommend using at least 3 cores per sample: two or more cores from the periphery of tumor and one core from the center since the highest Ki-67 index was seen in the tumor center in a third of the cases.

1683 BAC Array-Based Comparative Genomic Hybridization Utilizing Formalin-Fixed Paraffin-Embedded Tumor Specimens in Multiple Myeloma

DM Pierson, PA Lennon, C Williams, X Zhang, P Lin. MD Anderson Cancer Center, Houston, TX; PerkinElmer Inc., Waltham, MA.

Background: Conventional cytogenetic analysis in multiple myeloma (MM) is often non-informative given low mitotic activity of plasma cells (PC). Array-based comparative genomic hybridization (aCGH) has been shown to enhance detection of genomic aberrations. However, the utility of aCGH using formalin fixed paraffin-embedded (FFPE) samples is not well known.

Design: Paired fresh bone marrow tissue (FT) and corresponding FFPE samples from 8 MM cases were analyzed by aCGH. PCs from Ficoll-Paqued bone marrow aspirate samples were selected by immunomagnetic beads labeled with CD138 antibodies (Miltenyi-Biotec). Extracted DNA was then analyzed using the 1 Megabase-Resolution Microarray containing 2,640 BAC clones (PerkinElmer). The Axon microarray scanner (GenePix 4000B, Molecular Devices, Sunnyvale, CA) acquired image files and quantitation was done using GenePix Pro 6 software or BlueFuse software (BlueGnome Limited, Cambridge, UK).

Results: 7 of 8 paired MM samples were successfully analyzed. A total of 34 aberrations were identified. Of these, 29/34 was found in both tissue types, yielding 85% concordance. Table 1 lists those aberrations detected in paired samples of at least 2 cases. Complete concordance was observed in 4 cases with gains or losses ranging from 3-7 per case. In the remaining 3 cases with partial concordance, discrepancy was limited to 1-2 incongruence between FT and FFPE samples per case.

Common Aberrations* Detected in Paired FFPE & FT MM Samples

Aberrations	Gain	7q	15q	19p	Loss	8p	13q
# of cases		3	2	2		2	5

*Chromosomal

Conclusions: Array-CGH demonstrates reliability for identification of genomic aberrations in easily retrievable FFPE samples. FFPE may be more advantageous in some cases with scanty or insufficient aspirate material.

1684 Comparison of Two Fluorescence In-Situ Hybridization Techniques for Detection of Lymphoma-Associated Chromosomal Translocations in Paraffin-Embedded Tissue

JN Punia, J Sanchez, A Adeyinka, RC Hawley. Henry Ford Hospital, Detroit, MI.

Background: Detection of lymphoma-associated chromosomal translocations can facilitate diagnosis and classification of non-Hodgkin's lymphoma. Interphase fluorescence in-situ hybridization (FISH) is useful for detection of these translocations, given its high diagnostic sensitivity and applicability to fixed paraffin-embedded tissue. FISH can be performed on paraffin-embedded material using either tissue sections or extracted nuclei. The section technique is simpler and preserves histologic architecture, whereas the nuclear extraction technique eliminates nuclear crowding, overlap and truncation and facilitates scoring. The aim of this study was to compare the efficacy of the two techniques for detecting t(14;18) in follicular lymphomas (FL), t(11;14) in mantle cell lymphomas (MCL), t(8:14) in Burkitt lymphomas (BL), and t(2;5) in anaplastic large cell lymphomas (ALCL).

Design: 10 cases of FL, 10 cases of MCL, 6 cases of BL, 2 cases of ALCL (ALK+), and 10 cases of reactive lymphoid hyperplasia were selected for analysis. Formalin-fixed paraffin-embedded excisional biopsies were utilized in all cases, and all lymphomas were histologically and immunophenotypically defined according to WHO criteria. Two cores were obtained from a representative area in a paraffin block from each case. 3-4um sections prepared from one core and smears containing a monolayer of nuclei extracted from the other core were examined by fluorescence microscopy following pretreatment and hybridization. Probe sets utilized were the LSI IGH/BCL2 (Vysis) for FL, the LSI IGH/CCND1 XT (Vysis) for MCL, the LSI IGH/MYC/CEP8 (Vysis) for BL, and the LSI ALK (Vysis) for ALCL.

Results: Concordant positive results were obtained with both techniques in 7 of 10 FL, 10 of 10 MCL, 5 of 6 BL, and both ALCL. Concordant negative results were observed with both techniques in 2 of 10 FL and 1 of 6 BL. Discordant results (section technique positive/nuclear extraction technique negative) were found in 1 of 10 FL. Reactive controls yielded negative results with both techniques. No technical failures were encountered.

Conclusions: Our results indicate that the two techniques have comparable sensitivity and specificity and are effective means of detecting the respective chromosomal translocations. Our experience confirms that processing is simpler with the section technique, and that scoring is easier with the nuclear extraction technique.

1685 Characterization of a Newly Developed Rabbit Monoclonal Antibody to Cytokeratin 7 (CK7) for Immunohistochemistry

W Qi, J Chu, D Zhou, S King, D Tacha. Biocare Medical, LLC., Concord, CA.

Background: Rabbit antibody, in combination with mouse antibody, is a powerful tool in immunohistochemistry (IHC) multiple staining for dignostic pathology. We have successfully produced a polyclonal antibody to cytokeratin 7(CK7), which showed superior in double-staining of tissues by comparing with commercial available antibodies. In this paper, we further describe results obtained with a novel rabbit monoclonal antibody. The selected antibody was assessed by IHC on variety of tissues to compare with our polyclonal antibody. The initial results showed that the sensitivity and specificity were equal to the polyclonal antibody.

Design: Rabbits were immunized with a peptide corresponding to C-terminus of CK7. Recombinant monoclonal antibodies were developed using a proprietary novel method (Mariposa Bioscience, Inc., Burlingame, CA). Antibodies were screened by ELISA against CK-7 peptide, and the specificity of antibody was verified by Western Blotting on Hela cell lysates, and IHC on formalin fixed paraffin-embedded sections (FFPE).

Results: One clone, designated as BC1 was selected and tested on verity of tissues. Its reactivity patterns were compared with our newly developed polyclonal antibody as well as other well-characterized mouse monoclonal antibodies K72-7 and OV-TL 12/30. BC1 was able to stain variety FFPE tissues, like ovarian cancer, lung cancer, but not colon cancer. The staining intensity was comparable to the counterpart CK7 polyclonal antibody with less background than mouse monoclonal K72-7 and OV-TL 12/30. The antibody detected a single 51 kDa band on Hela cell extracts, corresponding to CK7 protein. BC7 did not cross-with mouse and rat CK7, tested by IHC on tissue microarrays (TMA).

Conclusions: A new CK7 recombinant monoclonal antibody BC1, produced with a new technology, could be a powerful tool in application for diagnostic pathology, especially in distinguishing stomach and colon cancers from breast, lung and ovarian cancers by multiple staining. To the best of our knowledge, this is the first CK7 rabbit monoclonal antibody that has been developed.

Fig. 1. Immunohistochemical analysis of CK7 with a rabbit monoclonal antibody BC1

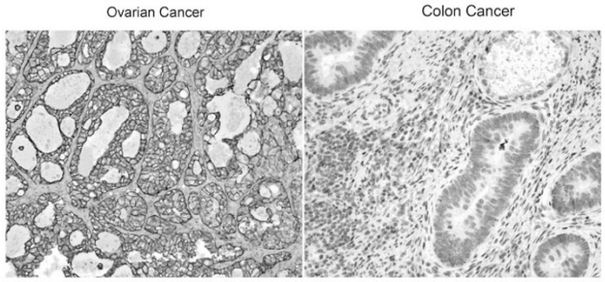

1686 Architectural Design of a Web-Based Scoring/Grading System for Non-Neoplastic Conditions: Bringing Simplicity to Diversity

ME Rodriguez, J Findeis-Hosey, D Hosey, Y Mao, Z Qu. Univeristy of Texas Medical School, Houston, TX; University of Rochester Medical Center, Rochester, NY.

Background: The reporting of non-neoplastic diseases can be more challenging than tumor synoptic reports because of infrequent encounters with the material and the diversity of the reporting elements. We developed a web-base scoring system enlisting multiple scoring/grading schemes to facilitate the reporting process and minimize scoring errors. However, because each grading schema is almost entirely different from others, it is very difficult to effectively add new schema or update the system.

Design: We used Microsoft Visual Web Development (VWD) to create a dynamic Microsoft Active Server Page (ASP.NET). We then created two databases as data sources for the dynamic web page. Generic data categories were created in the database fields using a combined alphabetical/numerical assignment. Scoring/grading schemes of diverse formats and data elements are entered under the generic categories in the database. The data presentation (i.e., web look) is controlled by a Visual Basic script.

Results: Reporting elements are presented as drop-down lists in the reporting templates by an internet browser. Specific scoring information can also be included as a reminder. The final report (including total scores) can be automatically generated based on the user's selection according to histological finding. The final report can then be incorporated into a pathology report in a laboratory information system by copy-paste. The web data components are permanently purged out when the browser is terminated. The system and reporting process are HIPPA compliant. Because of the architectural incorporation of database in the system, 1) the system provides diverse scoring schemes, 2) the reporting schemes are easy to modify, and 3) no additional programming or script is necessary when adding new schemes.

Conclusions: The improved reporting system not only makes routine pathology scoring/grading of diverse non-neoplastic diseases more efficient, but also makes it very easy to add new scoring schemes and/or update the contents and the output formats. The added flexibility of the system greatly enhances the usability of the system and minimizes technical demands on system maintenance.

1687 Expression Microdissection: A New Immuno-Based Dissection Technology for Cellular and Nuclear Procurement

J Rodriguez-Canales, ZK Majumdar, EC Ory, JC Hanson, TJ Pohida, MA Tangrea, RF Chuaqui, RF Bonner, MR Emmert-Buck. NCI, Bethesda; NICHD, Bethesda.

Background: Expression Microdissection (xMD) is an immuno-based dissection technology under development at NIH for rapid, specific, and semi-automated tissue microdissection. xMD is performed by identifying target cells in histological sections using immunohistochemical staining, covering the slide with a film, irradiating the entire field, and then removing the film with the captured cells. Used in concert with the relatively large number of available antibodies, xMD should permit investigators to efficiently recover cell types and sub-cellular components under a variety of biological and pathological conditions.

Design: Prostate tissue slides immunostained for keratins (AE1/3) for epithelial cell targeting, histone for general nuclear labeling, and p63 for basal cells nuclei labeling were employed. Diaminobenzidine was used as chromogen. A range of laser parameters were applied for tissue section irradiation using a 300mW, 473 nm, fiber optic coupled laser diode source with 120 uM spotsize. Dissection efficiency was assessed by analyzing the xMD film and histological section using light microscopic examination (LM), confocal imaging (CI) and scanning electron microscopy (SEM). As a molecular correlate, DNA was extracted from a subset of samples and analyzed for methylation of *GSTP1* promoter.

Results: Optimal staining showed an optical density ranging from 0.3-0.7 with a non-specific background ⟨0.05. A dissection scan rate of ~50,000 cells/sec was achieved when targeting epithelium in 1cm2 area using 140 mW and 1 scan per region at 80 mm/sec. LM examination of the dissected samples confirmed the purity of recovered epithelium with virtually no pickup of unstained regions. Pyrosequencing from these samples showed 9% *GSTP1* methylation in normal glands and 68% in tumor. Nuclear dissections were successfully performed for whole nuclei using histone antibody and basal cell nuclei using p63. 2 scans per region were used at 55 mm/sec with 140 mW power. LM, CI, SEM and DAPI fluorescence staining all showed consistent nuclear transfer to the xMD film and the presence of DNA in the dissected nuclei.

Conclusions: xMD facilitates procurement of cells and nuclei from tissue samples in a high-throughput and efficient manner. Further development of this technology may prove useful to investigators who require rapid and semi-automated dissection of cells and sub-cellular organelles.

1688 Comparison of the Qualitative Restriction Enzyme Based Assay to the Real-Time Quantitative Polymerase Chain Reaction Assay for Detection of the JAK2-V617F Mutation

S Sandhu, CK Huang, DH Fox, Q Pan. Montefiore Med Ctr/Albert Einstein Coll Med, Bronx, NY.

Background: The V617F mutation of the JAK2 (Janus kinase 2) gene is present in many patients afflicted with clonal hematological malignancies classified as myeloproliferative disorders (MPD). Restriction enzyme based polymerase chain reaction (RFLP-PCR) is a widely used qualitative assay for its detection. We compared the performance of the recently described, quantitative real-time PCR (Q-PCR) method.

Design: 183 consecutive clinical diagnostic samples previously sent for detection of the JAK2-V617F mutation and analyzed by the RFLP-PCR (InVivoScribe Tech), were selected. Extracted DNA from peripheral blood (PB) or bone marrow (BM) was stored at -80 C until analysis was performed by the Q-PCR using primers and probes from Kroger N. et al., Blood. 2007;109:1316-1321. The RFLP-PCR results were reported as **positive** or **negative**, based on the presence or absence of the 267bp amplicon product of digestion. For the Q-PCR, two simultaneous reactions were done with patient samples, one for the JAK2 and another for the hematopoietic cell kinase (HCK) as a control gene. ΔΔct method was used for percentage calculations. The results with detectable mutant allele were marked **positive and quantified** if the level was above >0.01% and ct value <42.

Results: A positive cell line DNA was diluted into a negative cell line DNA and reproducible results were obtained at the level of 0.01%. We set this as the sensitivity of the test. Of the total 183 samples, results were concordant for all the 38 **positive** and 133 out of 145 **negative** samples. 12 (6.55%) **negatives** by the RFLP-PCR, became **positive** by the Q-PCR. On revisiting clinical information, all 12 cases were found to have clinical evidence suspicious for MPD. Of 6 BM samples, 5 had megakaryocytic hyperplasia, 1 had left shift in myeloid maturation. Of 6 PB samples, 3 had thrombocytosis, 1 erythrocytosis, 2 erythrocytosis and granulocytosis. These clinical findings correlated with our Q-PCR results.

Conclusions: We compared two assays, RFLP-PCR with 5% sensitivity and Q-PCR with 0.01% sensitivity. All 38 previously positive samples were positive and of the 145 negative samples, 12 were positive by the new method which correlated with the clinical findings, thus proving that Q-PCR is more sensitive than RFLP-PCR.

1689 Computer-Assisted Grading of Follicular Lymphoma: High Grade Differentiation

O Sertel, J Kong, G Lozanski, A Shanaah, A Gewirtz, F Racke, J Zhao, U Catalyurek, JH Saltz, M Gurcan. The Ohio State University, Columbus, OH.

Background: Follicular Lymphoma (FL) is one of most common B cell malignancies. WHO recommends histological grading of FL that is based on the number of centroblasts per microscopic high power field (HPF) of 0.159 mm^2 manually counted in ten random HPFs. Unfortunately, this qualitative method is prone to sampling bias and inter- and intra-reader variability. Therefore, we are developing a fully automated image analysis system for the histologic grading of FL.

Design: In this study, we focused on differentiating the low and intermediate grades (I and II) from high grades (III). We used the ratio of the amount of cytoplasm to the amount of nuclei as a discriminative feature to distinguish low- and mid-grade tissues from high-grades. Therefore, we applied an automated segmentation algorithm to partition the images into several cytological components using an unsupervised clustering algorithm in the LAB color space. A consensus of five board-certified hematopathologists was used to determine the grade of 17 H&E stained whole-slide images. Two experienced pathologists extracted ten HPF regions from each of these slides and recorded the grade for each of 340 resulting images.

Results: Figure 1 (a) and (b) shows a sample image and its segmentation result obtained from a grade I FL image and (c) shows the histogram of cytoplasm to nuclei ratio for different grades. Although, the histogram of the ratio values that correspond to low- and mid-grades completely overlap, high-grade cases can be easily discriminated. The threshold value between low and high grades was determined using the Bayes optimality. The resulting sensitivity and specificity values on the training, testing data were 98.9%, 97.9% and 99.6%, 98.6%, respectively.

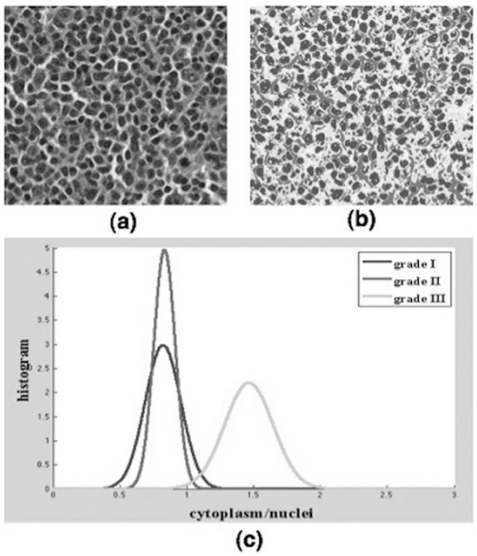

Conclusions: The computerized system provided promising results to differentiate low- and mid-grade FL cases from high-grades. The fully automated system can indicate high-grade regions in a whole-slide using rigid and highly reproducible criteria; therefore help preventing sampling bias and virtually eliminating inter- and intra-reader variability.

1690 The Role of Multispectral Microscopy in Differentiating Benign and Malignant Thyroid Nodules: A Pilot Study of 24 Cases

S Shah, MR Schwartz, DR Mody, M Scheiber-Pacht, M Amrikachi. The Methodist Hospital, Houston, TX; University of Houston, Houston, TX.

Background: Fine needle aspiration (FNA) is the recommended initial screening test for the diagnosis of thyroid nodules. In 10-15% of the cases, FNA reveals a follicular neoplasm with triage to surgical resection. Most of these neoplasms turn out to be benign. Several immunohistochemical and molecular markers have been suggested as potential tools in differentiating malignant from benign lesions. However, no single marker has been proven useful in this distinction. Multispectral microscopy allows for the measurement of the wavelength spectrum (transmitted or emitted) at every pixel of a two-dimensional image. We analyzed the role of this technique in differentiating benign and malignant thyroid lesions.

Design: A Czerny-Turner type monochromator, with a wavelength range of 400-700nm, connected to an Olympus BX51 upright optical microscope was utilized. A Photometrics SenSys™ CCD camera was used for high resolution, low light image acquisition. 24 thyroid FNA cases with subsequent surgical resection were selected. Cytologic diagnoses were benign in 4 cases, suspicious for neoplasm in 15 cases, malignant in 5 cases. For each case, a Papanicolaou-stained slide was analyzed by multispectral microscopic imaging, without knowledge of the final histopathologic diagnosis. Absorption parameter was calculated for each isolated cell. This computation was performed for 31 wavelengths in 10nm bands, resulting in 31 spectral measures per cell. Three different algorithms were used for automated differentiation between benign and malignant cases.

Results: Of 15 cases with suspicious cytologic diagnosis, 4 were malignant on surgical follow-up and 11 were benign. Multispectral analysis correctly predicted that 10 cases were benign and 3 cases were malignant. There was one false positive and one false negative result. Using these computerized algorithms, 87.5% of the 24 FNAs were correctly diagnosed. By combining spectral and morphologic features, correct diagnoses were reached in 92.7% of the cases.

Conclusions: Preliminary data shows the use of multispectral analysis along with morphometric information may improve our diagnostic ability. This novel computerized system appears to be of added value in the evaluation of suspicious thyroid FNAs. Further evaluation of this technique on a larger cohort of patients is warranted to confirm the utility of this technique in the diagnosis of thyroid nodules.

1691 Digital Imaging and Its Implementation and Utilization at a Large Academic Multi-Institutional Center

SJ Sirintrapun, R Anderson, J Duboy, A Ishtiaque, J Ho, JL Fine, DM Jukic, AV Parwani. University of Pittsburgh Medical Center, Pittsburgh, PA; University of Pittsburgh, Pittsburgh, PA.

Background: Digital pathology is increasingly being used in pathology practices. We provide our experience in the various practical uses as it relates to digital images such as whole slide imaging and telepathology.We also delve into the logistical and technical concerns for implementing such technologies.Finally we provide our hopes for future development.

Design: Static "snapshot" images are captured at microscopes and grossing workstations. SPOT Insight digital cameras capture both microscopic images at more than thirty locations and grossing images at six different locations.These static images are integrated into our APLIS (CoPathPlus).The Trestle DSM and Aperio Scanscope scanners are used to scan entire whole slides. With capture, image file sizes are approximately 2.7 GB.Conferences use telepathology through webcast or transmission with the Tandberg video system.Frozen section diagnoses can be made remotely through robotic means via Apollo,Trestle,and Nikon Coolscope systems.

Results: Over 350,000 static images have been captured,using 70 GB of server storage space.Static images are used for teaching,CPC conferences,publications, image-enhanced reporting,and consultation.We have a repository of over 5000 whole slide images;categorized and available through a centralized web-based portal.Whole slide imaging has increasingly been used in quality assurance,retrospective case review,and consultation.Telepathology has been integral to our educational conferences given our institutional geography.Conferences are video recorded with live broadcasts which permit remote attendance via the internet.More than 1000 conferences have been archived since 2002.Robotic telepathology has been actively used by transplant and neuropathology to make frozen section diagnoses.

Conclusions: Digital pathology has been successfully used for teaching, CPC conferences, QA/QC, publications, image-enhanced reporting,consultation,retrospective case review,frozen-section diagnosis,and advanced image analysis.Future goals and development in digital pathology include image capture and image analysis especially with immunohistochemistry and FISH.We hope to streamline the process even further so that all slides are imaged in their entirety.Our efforts hope to ensure that we reside on the forefront of new digital imaging technologies.

1692 The Development of a Double Stain CDX2/CK7 Cocktail for Routine Immunostaining

D Tacha, W Qi, S King, K Bloom, A AKyshtoobayeva, A Wu, J Pastore, D Van Eych. Biocare Medical, Concord, CA; Clarient, Aliso Viejo, CA; VA Healthcare Network, Upstate New York, Albany, NY; Waukesha Memorial Hospital, Waukesha, WI.

Background: Metastatic adenocarcinomas of unknown primary site are a common clinical problem. Immunohistochemical algorithms such as CDX2 and CK7 can be helpful in detecting tumors of unknown origin. Recently, one-step double immunostain detection kits have been developed. The method requires the combination of primary mouse and rabbit antibody cocktail. The CDX2 + CK7 cocktail would be ideal for double stain applications. The authors decided to see if they could develop a rabbit anti-CK7 antibody and thus develop a CDX2 + CK7 cocktail for double stain applications.

Design: A peptide corresponding to C-terminus of CK7 was synthesized with an amino terminal cysteine to facilitate conjugation to keyhole limpet hemocyanin (KLH). The peptide was conjugated to KLH. Two New Zealand white rabbits were immunized and antisera were tested by ELISA for reactivity against a CK7 peptide. CK7 positive sera was affinity purified and then compared with a mouse monoclonal CK7. A variety of tissues were tested including lung, breast, colon, ovarian and prostate cancers. CDX2 and CK7 were optimally titered and combined in an antibody cocktail. The antibody cocktail was detected using a cocktail of anti-mouse horseradish peroxidase and anti-rabbit alkaline phosphatase. The CDX2 and CK 7 were visualized with DAB and Fast Red chromogens respectively. CDX2 + CK7 cocktail was sent to participating beta sites for further testing.

Results: There were no staining discrepancies observed between the CK7 mouse monoclonal and CK7 rabbit polyclonal antibodies. In certain cases, staining patterns with the polyclonal CK7 were more specific and cleaner when compared with the mouse monoclonal CK7. The CDX2 + CK7 double stain was precise (Fig 1) and stained equally well when compared to individual stains. All beta sites laboratories confirmed similar results and gave favorable reviews.

Conclusions: CDX2 can be practically combined with CK7 as a double immunostain in the work-up of adenocarcinoma of unknown origin. This double stain is precise, cost effective and time efficient.

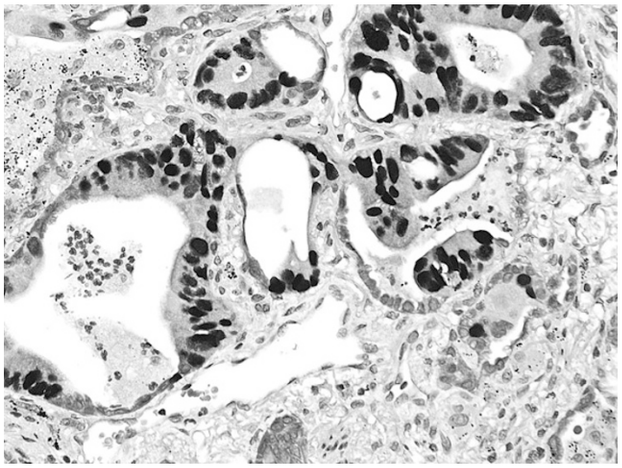

1693 Comparison of Two Phenotypic Screening Methods for the Detection of Blood-Borne AmpC B-Lactamase (AmpC) Producing Isolates

BM Turner, KH Rand. University of Florida, Gainesville, FL.

Background: The National Committee for Clinical Laboratory Standards does not currently require AmpC detection testing. Two simple methods for the detection of the AmpC enzyme are the AmpC disk test (ADT), based on the enzymatic inactivation of cefoxitin (Black et al, 2005), and the modified Hodge test (HT), based on the definitive growth of an indicator organism into an inhibition zone of cefoxitin along the test strain (Yong et al, 2002). These methods have so far only been performed with well characterized laboratory strains of *E. coli* and *K. pneumoniae*, and there is no study to date comparing these two methods.

Design: We tested 115 sequential gm- blood cultures (including *E. coli, K. pneumoniae*, *Enterobacter sp., P. mirabilis and P. aerugonisa*) for the presence of AmpC, with both the ADT and the HT. Testing was performed as previously described. The results were read independently by two observers.

Results: There was 92% (106/115) interobserver agreement between the ADT and HT. The ADT was positive 94% and 81% of the time when the HT was positive with observer 1 and 2, respectively. *All* interobserver discordance occurred when the HT positive results were less than 3mm definitive growth. Yong et al (2002) have suggested criteria of 3 mm definitive growth for interpreting a positive HT. Using a strict definition of 3mm for the HT, the ADT was positive 100% and 100% of the time when the HT was positive with observer 1 and 2, respectively. The HT was positive 71% and 74% of the time when the ADT was positive with observer 1 and 2, respectively. *All* interobserver discordance occurred with a weak positive ADT result. There are currently no quantitative criteria for interpreting a weak positive ADT.

Conclusions: AmpC remains a poorly defined resistance mechanism of clinical importance. Laboratories may report false in vitro susceptibility, particularly to 2nd and 3rd generation cephalosporins. Pai et al (2004) showed that the mortality of bloodstream infections of AmpC containing *Klebsiella sp.* was comparable to that of ESBL containing strains. These observations reinforce the need for simple phenotypic methods that can effectively detect AmpC in the hospital clinical laboratory. Both the ADT and the HT are easy to perform, correlate well with each other, and are candidates to fill this role. In addition, the HT defines quantitative criteria for a positive result that may help to better define weak positive results with the ADT. Molecular analysis of discordant results and correlation of these tests with clinical outcome will be of great interest.

1694 Quantitative Image Analysis of HER2 Immunohistochemistry Compared with Manual Pathologist Analysis in Breast Cancer

G Turner, G Kronauer, KJ Kaplan. Northwestern University Feinberg School of Medicine, Evanston, IL; Johns Hopkins University, Baltimore, MD.

Background: Use of image analysis (IA) is becoming more prevalent for routine clinical use in surgical pathology for increased quantification of diagnostic features that guide patient therapy. Whole slide images (WSI) allow for pathology slides to be converted into a digital data set that can be analyzed in its entirety with IA applications. Routine use of HER2 IHC staining is complicated by variations within tissue sections, tumor types and intra- and interobserver variability and workload related issues that may impact interpretation and patient management. We evaluated the use of IA in WSI for HER2 IHC in breast carcinomas.

Design: The LIS was searched for "FISH" and "HER2" for cases in 2006. 212 cases were retrieved of which 81 cases had original HER2 IHC slides available for review and scanning. The entire slide was scanned using an Aperio ScanScope® CS (Aperio Technologies, Inc., Vista, CA) scanner and analyzed using the provided membrane staining algorithm. Appropriate negative and positive controls were also analyzed for quality assurance. The results of image analysis and of manual semi-quantitative pathologist analysis (MA) were compared.

Results: Compared with FISH testing (amplified or non-amplified), IA for HER2 scoring was more accurate than MA in 55/81 cases (68%). All of these cases were scored as 2+ by MA and 1+ by IA and were non-amplified by FISH testing. MA was more accurate than IA in 12/81 cases (15%). Of these cases, 8 cases appeared to be overscored as 3+ by IA (8/8 cases FISH non-amplified originally scored as 1 or 2+ by MA) and 4 cases were underscored as 1+ compared with MA scores of 3+ (4/4 cases FISH amplified). IA

and MA yielded the same HER2 score in 14/81 cases (17%). All cases retrieved were scanned with an average scan and processing time of approximately 22 minutes.
Conclusions: Compared with FISH, IA of HER2 IHC appears to be more accurate than MA in a majority of cases, particularly with MA scores of 2+ on IHC with scores of 1+ by IA and non-amplified FISH testing. The algorithm in a minority of cases over scored or under scored the IHC results compared with MA, particularly in 3+ IHC cases by MA. This pilot study suggests there may be a role for IA, particularly in cases scored as 2+ by MA to eliminate unnecessary costs associated with FISH evaluation. Cost and time required for WSI analysis may still be prohibitive for routine clinical use without added resources in the laboratory for IA.

1695 Diagnostic Utility of Raman Molecular Imaging (RMI) in Separating Renal Oncocytoma from Chromophobe Renal Cell Carcinoma

AH Uihlein, S Stewart, J Maier, J Cohen, YL Liu, JF Silverman. Allegheny General Hospital, Pittsburgh, PA; ChemImage, Corp., Pittsburgh, PA.
Background: Raman Molecular Imaging (RMI), a technique used primarily in chemical analysis, is based on the scattering of laser light. We applied RMI as a reagentless tissue imaging approach to the analysis of pathology specimens. RMI yields an image of a sample wherein each pixel of the image is the Raman spectrum (RS) of the sample at the corresponding location. The RS generates data reflecting the local chemical environment of the sample at each location. RMI has a spatial resolving power of 250 nm and can potentially provide qualitative and quantitative image information based on molecular composition and morphology. We investigated the application of RMI on renal neoplasms that have overlapping histopathologic features.
Design: Our study evaluated whether RMI can be used to differentiate renal oncocytoma (OC) from chromophobe renal cell carcinoma (ChRCC). Raman images were generated from unstained sections of 10 OC and 10 ChRCC. Measurements derived from RMI of tissue samples were analyzed using multivariate techniques established in analytical spectroscopy. We applied Mahalanobis Distance Analysis (MD), a chemometric method that measures distance between data sets in RS for our study.
Results: Establishing ChRCC and OC as two different classes, and performing Principal Component Analysis (PCA) of the 68 spectra derived from RMI of the samples, allows calculation of MD between the two classes. This evaluation shows a clear distinction between ChRCC and OC data. A two-sample z-test applied to the PCA scores has a *p value* of less than 0.01, confirming a significant difference between the two renal neoplasms. All cases of ChRCC and OC were confirmed based on histopathologic findings and previously published molecular studies.
Conclusions: RMI shows potential to distinguish renal oncocytoma from chromophobe renal cell carcinoma which can often have challenging overlapping histologic features. We believe that RMI represents a novel analytical technique that may be able to assist pathologists in better classifying neoplasms that are not definitively distinguishable using traditional pathologic methods.

1696 Optimal Protein Extraction from Formalin-Fixed Paraffin-Embedded Tissues for Expression Profiling of Tumors

VA Valera, BA Walter, MJ Merino. National Cancer Institute, Bethesda, MD.
Background: Consistent results of using formalin-fixed paraffin-embedded (FFPE) tissues for protein analysis have been hampered by the lack of a reliable method for protein extraction. A successful technique for the solubilization of non-degraded and immunoreactive proteins from FFPE tissues would render an extraordinary opportunity to unlock the wealth of information from tissue collections with attached clinical and outcome data avilable worldwide.
Design: The application of different solubilization strategies and the principle of antigen retrieval were combined to extract proteins from FFPE tissue slides following a standard microdissection protocol. A dedicated software for experiment design (Design-Expert® ver. 7.1) was used to predict the optimal combination of factors that would yield the highest amount of extracted protein based on a factorial model of variables with several levels for each factor. Estimation of all main effects and all interaction effects was statistically tested by ANOVA and significance was defined as $p<0.05$. The quality of the extracted protein was tested by gel electrophoresis and western immunoblot analysis. Finally, the peptides and proteins identified from formalin-fixed tissue were then compared with those identified from frozen-fresh tissue.
Results: The quantity of extracted protein with all buffers varied from 9.54 up to 557.34 $ug.ml^{-1}$. When the amount of protein was related to the area of tissue microdissected, the mean value was 1.4 $ug \cdot ml^{-1}$ per mm^2 of tissue (range 0.51-2.25). There was no significant difference for the amount of extracted protein between FFPE samples and those obtained from fresh tissue using the same buffers, (mean concentration: 389.72 vs. 341.84 $ug \cdot ml^{-1}$, $p=0.600$). The software predicted that the combination of high concentration of detergent (2% SDS) and heating for 120 minutes at 95°C would give the highest yield of protein for the 60 potential combinations of factors after analyzing few preliminary results. Western blot analysis confirmed that the extracted proteins were present and immunoreactive similar to those obtained from frozen tissues.
Conclusions: An optimal combination of heat, detergent and ionic strength in the extraction buffer is necessary for maximal protein recovery from FFPE tissues. With this method, valuable protein information could be obtained similar to those from frozen tissues, and represents an alternative approach for disease biomarker analysis or when biomarker quantitation is needed.

1697 A Simple and Inexpensive Method for the Construction of Paraffin Tissue Microarrays from Needle Biopsy Specimens: Example with Breast Needle Biopsy Specimens

UF Vogel, BD Bueltmann. University Hospital, Eberhard-Karls-University, Tuebingen, Baden-Wuerttemberg, Germany.
Background: Paraffin tissue microarrays (PTMAs) as introduced by Kononen et al. in 1998 are a well-established technique in pathological research and even for pathological routine work. Customarily, paraffin tissue core biopsies (PTCBs) from paraffinized resection material are used for the construction of the PTMAs. However, sometimes needle biopsy specimens (NBSs) are the only material of a patient who might be treated by nonsurgical methods such as radiation, chemotherapy, or palliative care. Moreover, it is unescapable to study the NBSs if the immunoprofile of a tumor should be examined before and after chemotherapy in a neoadjuvant setting. Therefore, we looked for a simple and inexpensive technique to construct PTMAs using NBSs.
Design: Routine Hematoxylin-Eosin stained slides of 94 breast NBSs were screened for those areas where the tissue of interest (carcinoma) was equally disseminated within a 4 mm long section. These parts of the NBSs were punched of the paraffin block using a 4 mm in diameter biopsy punch, melted in a routine steel mold, picked up with a 25-gauge needle and manually transferred to the holes of a predrilled recipient block (PTMA: number of the holes: 150; diameter of the holes: 1.4 mm; distance of the holes: 0.3 mm). When all the holes were filled, the PTMA was cut with a rotary microtome to ensure that the PTCBs reached the surface of the PTMA to get contact to a double-sided adhesive tape. Then the PTMA was melted on a standard hot plate at 65°C in a metal mold to ensure a strong contact between the PTCBs and the surrounding paraffin. During this melting procedure the PTCBs were held in place by the adhesive tape. Cutting, staining and evaluation were performed according to routine procedures.
Results: A PTMA with 84 PTCBs of NBSs could be successfully constructed. There was no difference in cutting, staining and evaluation of the sections in comparison to PTMAs made of resection material. About 11% of the originally screened 94 NBSs were not punched due to a patchy distribution of the carcinoma. On the average 15% of the PTCBs used in the PTMA were non-informative mostly due to missing tumor cells when evaluating the different immunohistochemical stainings (e.g. estrogen receptor).
Conclusions: With this simple and inexpensive method it is possible to use NBSs for the construction of PTMAs like resection specimens and to make NBSs accessible for high throughput examinations.

1698 Paraffin Tissue Microarrays Constructed with a Cutting Board, a Board of Steel Spacers and a Soldering Iron

UF Vogel, BD Bueltmann. University Hospital, Eberhard-Karls-University, Tuebingen, Baden-Wuerttemberg, Germany.
Background: The construction of paraffin tissue microarrays (PTMAs) consists of putting paraffin tissue core biopsies (PTCBs) from donor blocks (e.g. paraffin tissue blocks of daily pathological work) into preformed holes of recipient blocks (formerly blank paraffin blocks). Because of the different thickness of the tissue in the donor blocks the PTCBs are of different length. In consequence, the sections of the deeper portions of the PTMA do not contain all of the PTCBs thereby diminishing the efficacy of the PTMA technique.
Design: To overcome this drawback and to cut the PTCBs to a certain length we manufactured a cutting board (3) out of plexiglass with a thickness of 4 mm. 144 holes were drilled into this board which were filled completely by at least one PTCB. Those PTCBs which stand over the surface of the cutting board were cut with a sharp knife. These cut parts were installed again in other holes of the cutting board or stored in microtubes for further PTMAs or other investigations like morphological-independent PCR. The holes of the PTMAs were poured in advance using a board equipped with 144 steel pins as spacers (1+2). When the holes of the cutting board were filled the PTCBs were injected simultaneously from the cutting board into the holes of a PTMA using the board of steel pins (1+2+3). Then, the paraffins of the PTMA and the PTCBs were melted using a soldering iron to ensure a solid contact of the paraffins.

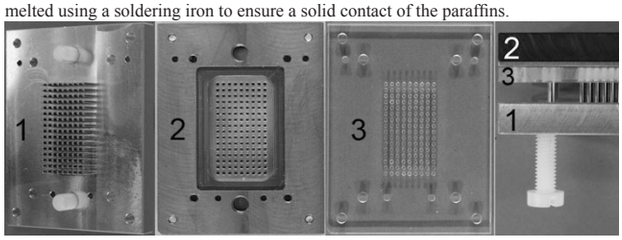

Results: Several PTMAs were constructed and cut with a standard rotary microtome. Per PTMA up to 1000 sections could be obtained which comprised nearly all of the 144 PTCBs.
Conclusions: Using the cutting board, the board of steel spacers and the soldering iron it was possible to construct efficiently PTMAs which did not show the thinning out of PTCBs in deeper sections.

1699 Evolutionary Concepts in Biobanking: The BC BioLibrary

PH Watson, JE Wilson-McManus, RG Hegele, IR Mackenzie, DG Huntsman. University of British Columbia, Vancouver, BC, Canada.
Background: The limited availability of annotated and adequately-collected biospecimens is creating a growing gap between the pace of scientific and technological advances and successful knowledge exploitation to further the goal of prevention or cure of human disease. Biobanks are collections of biospecimens (BSp) (tissues, blood, body fluids) and their associated clinical and outcome data. Research biobanks (clinical trial or basic research studies; disease-affiliated banks) have evolved significantly outside pathology and incorporate well-developed standards for donor consent, BSp

processing protocols, and advanced databases, in comparison with clinical biobanks. One emerging strategy to enhance quality and capacity in research biobanking is to 'repatriate' aspects to pathology.

Design: The British Columbia (BC) BioLibrary model (figure 1) combines: 1) specialized BSp collection units (BCU) embedded within clinical pathology departments with trained personnel, 2) a BSp catalogue of consented research study donor lists, 3) a BSp distribution system in parallel with analysis capacity, and 4) oversight through an interdisciplinary governance structure and molding by public deliberation.

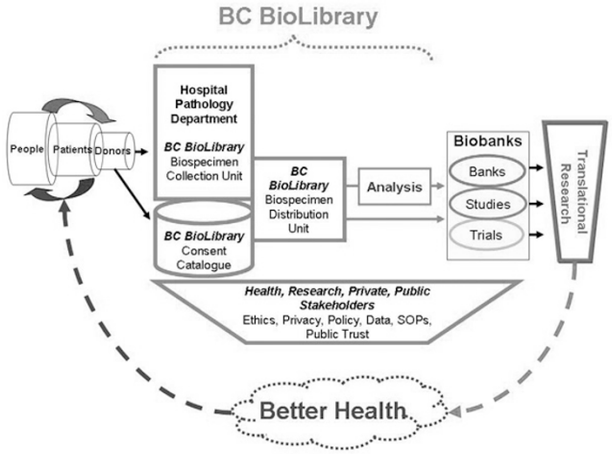

Results: The first BCU has been established and has collected more than 20 BSp. The BC BioLibrary is embraced by leaders in biobanking, pathology, and translational research, from multiple institutions, disease focused research groups and BC funding agencies. This success in engagement and support is driving a pilot phase that will also mold the final design and governance of the model.

Conclusions: The Biolibrary model is designed to maximize the injection of consented, high quality, annotated biospecimens into all forms of biobanks. An opportunity for oversight of biospecimen use, standardization of collection, and equity in distribution to biobanks is created. In the future, this model can promote the harmonization of consent processes and biobanking procedures for processing, storage, and annotation. By creating a common infrastructure, the model reduces competition between biobanks and the tissue providers, offers a transparent process for donors and enhances public trust in biobanking.

1700 Is ER and/or PR Expression Specific Enough To Confirm the Diagnosis of Metastatic Carcinoma of Breast or Gynecological Origin?

S Wei, N Said-Al-Naief, O Hameed. University of Alabama School of Medicine, Birmingham.

Background: Estrogen receptor (ER) and progesterone receptor (PR) are commonly expressed in breast and gynecological carcinomas, and are sometimes used to "confirm" the mammary origin of an adenocarcinoma at a metastatic site, especially when the primary tumor is positive for one or both of these markers. This is despite previous reports that have shown that a variable proportion of non-mammary/non-gynecological adenocarcinomas can also express ER, which would appear to limit their usefulness in this regard. The aim of this study was to systematically evaluate the frequency of ER and PR expression in various non-mammary/non-gynecological adenocarcinomas to further clarify this issue.

Design: Commercially available paraffin-embedded tissue microarrays (TMAs) of malignant tumors of a variety of human organ systems [78 primary lung carcinomas (34 adeno, 33 squamous cell, 1 sarcomatoid, 1 large cell, and 9 small cell), 72 gastric adenocarcinomas, 40 esophageal carcinomas (9 adeno, 29 squamous cell, 1 small cell and 1 sarcomatoid), 78 colonic adenocarcinomas, 20 renal cell carcinomas (clear cell type), and 20 urothelial carcinomas] were immunhistochemically stained for ER (clone 6F11, prediluted, Ventana) and PR (clone 1A6, prediluted, Ventana), with appropriately reactive negative and positive controls. Tumors were scored as positive when any unequivocal nuclear-staining was identified regardless of strength.

Results: Nuclear expression of ER or PR was not detected in any of the primary lung carcinomas, gastric adenocarcinomas, esophageal carcinomas, colonic adenocarcinomas, renal cell carcinomas, or urothelial carcinomas. While ER was not expressed, PR was detected in one case (1/40, 2.5%) of pancreatic ductal adenocarcinomas. Interestingly, PR immunoreactivity was occasionally found in normal stromal cells of bladder regardless of gender.

Conclusions: 1) Although some previous reports suggest otherwise, in the appropriate clinical and histological settings, the lack of ER and PR expression in the tissues evaluated in this study suggest that the addition of ER/PR to a panel of other markers may be particularly helpful in confirming the breast/gynecological origin of a metastatic carcinoma of unknown primary. 2) The lack of nuclear expression of ER/PR does not support these transcription factors having a significant role in tumorigenesis in these organ systems.

1701 Whole Slide Imaging Digital Pathology: A Pilot Study Using Paired Subspecialist Correlations

DC Wilbur, K Madi, RB Colvin, LM Duncan, WC Faquin, JA Ferry, MP Frosch, SL Houser, RL Kradin, GY Lauwers, DN Louis, EJ Mark, M Mino-Kenudson, J Misdraji, GP Nielsen, MB Pitman, A Rahemtullah, AE Rosenberg, RN Smith, JR Stone, RH Tambouret, C-L Wu, RH Young, A Zembowicz, W Klietmann. Massachusetts General Hospital, Boston, MA; University Federal de Rio de Janeiro, Rio de Janeiro, Brazil; Harvard Medical School, Boston, MA; Corista LLC, Concord, MA.

Background: Whole slide imaging technology offers promise for rapid Internet-based telepathology consultations between institutions. Technical issues, pathologist adaptability, and morphologic pitfalls inherent to this process have not been well characterized.

Design: Histopathology slides of diseases from a variety of anatomic sites with reference diagnoses were selected by an outside laboratory. Virtual slides were made using a Zeiss Mirax scanner. Virtual and glass slides were diagnosed independently by 2 subspecialty pathologists appropriate for each anatomic site. Reference diagnoses were compared to virtual and glass slide interpretations, and correlation data was tabulated. Comments on virtual slide technical issues were gathered.

Results: 53 cases were analyzed. There was agreement between virtual, glass, and reference diagnoses in 45 (85%), and between virtual and glass diagnoses in 48 (91%) cases. There were 5 virtual cases (9%) discordant with both reference and glass slide diagnoses. Further review of these cases indicated an incorrect virtual slide interpretation. By anatomic site, concordance rates between virtual and glass slide reviews were: lung - 89% (8/9), liver/GI tract - 82% (9/11), cardiovascular - 100% (5/5), hematopathology - 80% (4/5), thyroid/salivary gland - 100% (6/6), skin - 50% (1/2), kidney - 100% (6/6), prostate - 100% (1/1), gynecologic - 100% (4/4), bone and soft tissue - 100% (3/3), and neuropathology - 100% (1/1). Neoplastic cases showed better correlation (93%) than did cases of non-neoplastic disease (88%). Comments on discordant cases related to virtual slide technical issues such as fine resolution and navigating ability at high magnification.

Conclusions: Overall concordance between virtual and standard slide interpretations was good at 91%. Adjustments in technology, case selection, and further experience to include identification of pitfalls and technology familiarization should improve performance, making digital whole slide review feasible for broader telepathology application.

Ultrastructural

1702 Use of Electron Microscopy in Core Biopsy Diagnosis of Oncocytic Renal Tumors

NA Belsley, MM Johnson, MK Selig, GP Nielsen. Beth Israel Deaconess Hospital, Boston; Massachusetts General Hospital, Boston.

Background: Renal tumor biopsies are being performed more frequently, with the increased detection of small lesions and the use of minimally invasive therapies like radiofrequency ablation (RFA). Distinction between oncocytoma (OC) and chromophobe renal cell carcinoma (CR) on core biopsy is important to guide management. At one of our institutions (MGH), CR is resected or ablated, whereas OC may be clinically followed, with indeterminate lesions treated as CR. Our aim was to evaluate the use of electron microscopy (EM) in distinguishing between OC and CR on needle core biopsies.

Design: The MGH case files were searched for renal core biopsies with a diagnosis of OC, CR or granular cell tumor, indeterminate (GT). Cases in which paraffin blocks were unavailable or in which there was insufficient tissue for EM were excluded. H&E-stained slides as well as any special stains (*i.e.* colloidal iron) or immunohistochemical stains (IC) ordered were reviewed. EM on formalin-fixed, paraffin-embedded tissue was then performed and used as the gold standard to measure the sensitivity and specificity of renal biopsy in differentiating OC from CR.

Results: Fifty-five biopsies of granular cell tumors were identified. After excluding those with unavailable blocks or insufficient tissue for EM, 20 cases remained. Of these, 13 (65%) cases carried a diagnosis of OC, 4 (20%) of CR and 3 (15%) of GT. Diagnosis was aided by colloidal iron in 11 cases, by IC in 2 cases and by EM in 3 cases. By EM, 6 CRs (3 CRs, 1 OC and 2 GTs by initial review) and 14 OCs (1 CR, 12 OCs and 1 GT by initial review) were diagnosed. Ultrastructural detail was variable, but diagnoses were confidently rendered on all cases by two microscopists. The sensitivity and specificity without routine EM (excluding GCT) was 75% and 92%, respectively. Five patients underwent resection, confirming the EM diagnosis, and 3 patients had RFA. No further follow-up was available.

Conclusions: OC and CR can be difficult to differentiate, especially in a limited sample, as their histologic features often merge. Colloidal iron and IC may be of use, but with a clinical branch point of therapy versus follow-up, correct diagnosis is crucial. EM can be useful, even using small, formalin-fixed, paraffin-embedded tissue samples. In this study, one false negative and one false positive were revealed by EM; both were initially managed with RFA. With more certainty in diagnosing granular cell tumors, risk of treatment, cost of follow-up and patient anxiety can be diminished.

1703 Ultrastructural Characterization of Amyloidoma by Scanning and Transmission Electron Microscopy

CA Garcia, SI Gamb, DV Miller. University of Illinois - Peoria, Peoria, IL; Mayo Clinic, Rochester, MN.

Background: Amyloidomas are localized mass-forming deposits of amyloid that occur with or without association with systemic amyloidosis. Amyloidomas may contain AL, AA, senile, dialysis related, or heredofamilial forms of amyloid. Amyloidomas have been well characterized in terms of their histologic, histochemical, and immunohistochemical